(2)

David Taylor Research Center
Bethesda, MD 20084–5000

DTRC–90/009 April 1990
Propulsion and Auxiliary Systems Department
Research and Development Report

Propulsive Efficiencies of Magnetohydrodynamic Submerged Vehicular Propulsors

by
S. H. Brown, J.S. Walker, N.A. Sondergaard,
P.J. Reilly, and D.E. Bagley

MAJOR DTRC TECHNICAL COMPONENTS

CODE 011 DIRECTOR OF TECHNOLOGY, PLANS AND ASSESSMENT

12 SHIP SYSTEMS INTEGRATION DEPARTMENT

14 SHIP ELECTROMAGNETIC SIGNATURES DEPARTMENT

15 SHIP HYDROMECHANICS DEPARTMENT

16 AVIATION DEPARTMENT

17 SHIP STRUCTURES AND PROTECTION DEPARTMENT

18 COMPUTATION, MATHEMATICS & LOGISTICS DEPARTMENT

19 SHIP ACOUSTICS DEPARTMENT

27 PROPULSION AND AUXILIARY SYSTEMS DEPARTMENT

28 SHIP MATERIALS ENGINEERING DEPARTMENT

DTRC ISSUES THREE TYPES OF REPORTS:

1. **DTRC reports, a formal series,** contain information of permanent technical value. They carry a consecutive numerical identification regardless of their classification or the originating department.

2. **Departmental reports, a semiformal series,** contain information of a preliminary, temporary, or proprietary nature or of limited interest or significance. They carry a departmental alphanumerical identification.

3. **Technical memoranda, an informal series,** contain technical documentation of limited use and interest. They are primarily working papers intended for internal use. They carry an identifying number which indicates their type and the numerical code of the originating department. Any distribution outside DTRC must be approved by the head of the originating department on a case-by-case basis.

NDW-DTNSRDC 5602/51 (Rev 2-88)

REPORT DOCUMENTATION PAGE

1a. REPORT SECURITY CLASSIFICATION Unclassified	1b. RESTRICTIVE MARKINGS
2a. SECURITY CLASSIFICATION AUTHORITY	3. DISTRIBUTION/AVAILABILITY OF REPORT Approved for public release; distribution is unlimited.
2b. DECLASSIFICATION/DOWNGRADING SCHEDULE	
4. PERFORMING ORGANIZATION REPORT NUMBER(S) DTRC–90/009	5. MONITORING ORGANIZATION REPORT NUMBER(S)
6a. NAME OF PERFORMING ORGANIZATION David Taylor Research Center 6b. OFFICE SYMBOL (*If applicable*) Code 271	7a. NAME OF MONITORING ORGANIZATION
6c. ADDRESS (*City, State, and ZIP Code*) Bethesda, Maryland 20084–5000	7b. ADDRESS (*City, State, and ZIP Code*)
8a. NAME OF FUNDING/SPONSORING ORGANIZATION (See reverse side) 8b. OFFICE SYMBOL (*If applicable*) DTRC0113	9. PROCUREMENT INSTRUMENT IDENTIFICATION NUMBER
8c. ADDRESS (*City, State, and ZIP Code*) DTRC Bethesda, Maryland 20084–5000	10. SOURCE OF FUNDING NUMBERS PROGRAM ELEMENT NO. 62936N; PROJECT NO. 1–2712–131; TASK NO. ZF66412001; WORK UNIT ACCESSION NO. 500540

11. TITLE (*Include Security Classification*)

Propulsive Efficiencies of Magnetohdrodynamic Submerged Vehicular Propulsors

12. PERSONAL AUTHOR(S)

Samuel H. Brown, John S. Walker, Neal A. Sondergaard, Patrick J. Reilly, and David E. Bagley

13a. TYPE OF REPORT	13b. TIME COVERED	14. DATE OF REPORT (*YEAR, MONTH, DAY*)	15. PAGE COUNT
Final	FROM_____ TO_____	April 1990	64

16. SUPPLEMENTARY NOTATION This work was a cooperative effort with the Deparment of Maechanical and Industrial Engineering at the University of Illinois, Urbana Ill. 61801

17. COSATI CODES			18. SUBJECT TERMS (*Continue on reverse if necessary and identify by block number*)
FIELD	GROUP	SUB–GROUP	Magnetohydrodynamic propulsion, marine propulsion, seawater pump, superconducting magnets

19. ABSTRACT (*Continue on reverse if necessary and identify by block number*)

Magnetohydrodynamic (MHD) ship propulsion is the process of propelling a vehicular structure by a seawater electromagnetic pump. This propulsion system can be applied to a surface ship or a submerged vehicle; however, in this work only submerged vehicles at depths where wave effects can be neglected were considered. Although a number of different arrangements for a MHD propulsion system are possible, the general characteristics of such systems are most easily determined by a simple, ideal MHD rectangular duct of constant cross-sectional area. A mathematical model was developed ~~at the David Taylor Research Center~~ (DTRC) for calculating the propulsive efficiencies of such a rectangular duct propelling a submerged vehicle. Numerical propulsive efficiencies are presented in terms of many different parameters. Assumptions were generally made in the model that tend to maximize the propulsive efficiency of the MHD system. Thus, the propulsive efficiencies calculated from the model overestimate the efficiencies of the corresponding real MHD propulsion system. These numerical results can be used for engineering estimates of the propulsive efficiencies of real MHD propulsion systems.

(Continued on reverse side)

20. DISTRIBUTION/AVAILABILITY OF ABSTRACT	21. ABSTRACT SECURITY CLASSIFICATION
☐ UNCLASSIFIED/UNLIMITED ☒ SAME AS RPT ☐ DTIC USERS	Unclassified

22a. NAME OF RESPONSIBLE INDIVIDUAL	22b. TELEPHONE (*Include Area Code*)	22c. OFFICE SYMBOL
Samuel H Brown	(301)–267–2146	Code 2712

Block 8a:

DTRC Independent Research Program, Director of Naval Research;
Submarine Block Program, Office of Naval Technology

Block 13 (Continued):

A comparison of the ideal model MHD rectangular duct propulsive efficiencies with the corresponding efficiency of a conventional submerged vehicle propeller (order of 0.85) generally shows the MHD efficiencies to be less under most conditions. The cases where MHD propulsive efficiencies are in ranges that approach that of a propeller correspond to MHD duct volumes greater then 300 m^3, with small surface-area-to-volume ratios, or the magnetic inductions are in the order of 20 tesla or more. Magnetic inductions of about 6 to 10 tesla in large volumes of space, such as MHD ducts, are probably about the highest field strengths possible with the use of present-day superconducting magnet construction technology; to produce even these fields will require significant engineering effort in magnet construction. Therefore an important area of concern for MHD propulsion is the construction of practical superconducting magnets and support structures of reasonable mass.

According to the calculations using the mathematical model, a weakness of MHD propulsion, for a viable submerged vehicle propulsion system, is the generally low propulsive efficiencies of the system at duct magnetic inductions of 10 tesla or less, when compared with conventional propellers. Furthermore, the general trend is for propulsive efficiencies to decrease as vehicle speed increases. Future work will address the degrading effects on the rectangular MHD channel, caused by fringing magnetic induction and current distributions at the duct ends.

A very important and potentially promising aspect of MHD propulsion is the possible reduction of the submerged vehicle's acoustic noise signature. Unlike a propeller, the MHD duct has no mechanical moving parts. This may make the MHD propulsor intrinsically quieter (acoustically) than a rotating propulsor. Also, the replacement of the propeller by a MHD thruster eliminates the requirement for a high pressure rotating shaft seal. Therefore, in spite of the model's lower predicted propulsive efficiencies, the acoustic aspects of MHD propulsive should be investigated in detail, and the possibility of designing and constructing a practical, acoustically quiet submerged vehicle, even at the possible expense of propulsive efficiency, should be explored.

CONTENTS

	Page
Abstract	1
Administrative Information	2
Introduction	2
History	2
MHD Propulsion Concept	2
MHD Project Goals	2
Goals of this Technical Report	3
Traditional Propeller Theory and Approximate Extension to MHD Ducts	4
Background	4
Approximate Relationship of Propeller to MHD Duct	10
***Mathematical Model of Magnetohydrodynamic (MHD) Ship* Propulsion with Propulsive Efficiency**	13
Fundamental Equations of MHD Propulsion	13
Conservation of Linear Momentum	14
Principle of Action and Reaction	16
Rate of Change of Kinetic Energy (Energy Theorem)	17
Electromagnetic Energy Input	19
Efficiencies for MHD Propulsion	20
Numerical Results	22
Discussion and Conclusions	51
Acknowledgments	53
Appendix A. Three-Dimensional Effects	54
References	57

FIGURES

1. Stream tube for propeller system.	5
2. Control volume in space.	6
3. Control volume for propeller mathematical model.	7
4. Simple MHD rectangular duct.	10
5. MHD rectangular duct.	13
6. Propulsive magnetohydrodynamic rectangular duct configuration.	23
7. Power consumption versus submerged vehicle speed.	24

8. Propulsive efficiency of square MHD duct versus vehicle speed in meters per second. 26
9. Thrust required to propel submerged vehicle at constant speed V. 28
10. Propulsive efficiency of square MHD duct versus magnetic induction in tesla. 29
11. Propulsive efficiency versus electrical conductivity of seawater. 30
12. Propulsive efficiency of square MHD duct versus duct cross-sectional area. 31
13. Propulsive efficiency of square duct versus duct length. 32
14. Propulsive efficiency η_1 versus duct height (duct width w = 1 m) 34
15. Propulsive efficiency η_1 versus duct height (duct width w = 2 m) 35
16. Propulsive efficiency η_1 versus duct height (duct width w = 4 m) 36
17. Propulsive efficiency η_1 versus duct height (duct width w = 8 m) 37
18. Propulsive efficiency η_1 versus duct height (duct width w = 16 m) 38
19. Streamlines due to uniform body force JB distributed over rectangular volume with no duct walls 55

TABLES

1. Baseline numerical results for square rectangular duct 25
2. Propulsive efficiency $\eta_1 \times 10^2$ versus submerged vehicle speed and length of square duct at 2 tesla 39
3. Propulsive efficiency $\eta_1 \times 10^2$ versus submerged vehicle speed and length of square duct at 6 tesla 40
4. Propulsive efficiency $\eta_1 \times 10^2$ versus submerged vehicle speed and length of square duct at 10 tesla 41
5. Propulsive efficiency $\eta_1 \times 10^2$ versus submerged vehicle speed and length of square duct at 6 tesla 42
6. Propulsive efficiency $\eta_1 \times 10^2$ versus submerged vehicle speed and length of square duct at 10 tesla 43
7. Propulsive efficiency $\eta_1 \times 10^2$ versus electrical conductivity and submerged vehicle speed 44
8. Propulsive efficiency $\eta_1 \times 10^2$ versus electrical conductivity and magnetic induction of square duct 45
9. Propulsive efficiency $\eta_1 \times 10^2$ versus hydrodynamic resistance of submerged vehicle (hydrodynamic resistance $R = 1000\ V^2$ newtons). 46
10. Propulsive efficiency $\eta_1 \times 10^2$ versus hydrodynamic resistance of submerged vehicle (hydrodynamic resistance $R = 2000\ V^2$ newtons). 47

11. Propulsive efficiency $\eta_1 \times 10^2$ versus hydrodynamic resistance of submerged vehicle (hydrodynamic resistance $R = 3000\ V^2$ newtons) 48

12. Propulsive efficiency $\eta_1 \times 10^2$ versus hydrodynamic resistance of submerged vehicle (hydrodynamic resistance $R = 4000\ V^2$ newtons) 49

13. Propulsive efficiency $\eta_1 \times 10^2$ versus hydrodynamic resistance of submerged vehicle (hydrodynamic resistance $R = 5000\ V^2$ newtons). 50

ABSTRACT

Magnetohydrodynamic (MHD) ship propulsion is the process of propelling a vehicular structure by a seawater electromagnetic pump. This propulsion system can be applied to a surface ship or a submerged vehicle; however, in this work only submerged vehicles at depths where wave effects can be neglected were considered. Although a number of different arrangements for a MHD propulsion system are possible, the general characteristics of such systems are most easily determined by a simple, ideal MHD rectangular duct of constant cross-sectional area. A mathematical model was developed at the David Taylor Research Center (DTRC) for calculating the propulsive efficiencies of such a rectangular duct propelling a submerged vehicle. Numerical propulsive efficiencies are presented in terms of many different parameters. Assumptions were generally made in the model that tend to maximize the propulsive efficiency of the MHD system. Thus, the propulsive efficiencies calculated from the model overestimate the efficiencies of the corresponding real MHD propulsion system. These numerical results can be used for engineering estimates of the propulsive efficiencies of real MHD propulsion systems.

A comparison of the ideal model MHD rectangular duct propulsive efficiencies with the corresponding efficiency of a conventional submerged vehicle propeller (order of 0.85) generally shows the MHD efficiencies to be less under most conditions. The cases where MHD propulsive efficiencies are in ranges that approach that of a propeller correspond to MHD duct volumes greater then 300 m^3, with small surface-area-to-volume ratios, or the magnetic inductions are in the order of 20 tesla or more. Magnetic inductions of about 6 to 10 tesla in large volumes of space, such as MHD ducts, are probably about the highest field strengths possible with the use of present-day superconducting magnet construction technology; to produce even these fields will require significant engineering effort in magnet construction. Therefore an important area of concern for MHD propulsion is the construction of practical superconducting magnets and support structures of reasonable mass.

According to the calculations using the mathematical model, a weakness of MHD propulsion, for a viable submerged vehicle propulsion system, is the generally low propulsive efficiencies of the system at duct magnetic inductions of 10 tesla or less, when compared with conventional propellers. Furthermore, the general trend is for propulsive efficiencies to decrease as vehicle speed increases. Future work will address the degrading effects on the rectangular MHD channel, caused by fringing magnetic induction and current distributions at the duct ends.

A very important and potentially promising aspect of MHD propulsion is the possible reduction of the submerged vehicle's acoustic noise signature. Unlike a propeller, the MHD duct has no mechanical moving parts. This may make the MHD propulsor intrinsically quieter (acoustically) than a rotating propulsor. Also, the replacement of the propeller by a MHD thruster eliminates the requirement for a high pressure rotating shaft seal. Therefore, in spite of the model's lower predicted propulsive efficiencies, the acoustic aspects of MHD propulsive should be investigated in detail, and the possibility of designing and constructing a practical, acoustically quiet submerged vehicle, even at the possible expense of propulsive efficiency, should be explored.

ADMINISTRATIVE INFORMATION

This work was a cooperative effort between DTRC and the Department of Mechanical and Industrial Engineering at the University of Illinois, Urbana, Ill. 61801. The work was supported by the DTRC Independent Research Program, Director of Naval Research (OCNR10), and administered by the Research Director (DTRC0113) under Program Element 62936N, Task Area ZF66412001, Work Unit 1–2712–131, project title "The Fundamental Conceptual Design and Analysis of Magnetohydrodynamic Propulsors." In addition, this work was partially supported by the DTRC Block Program sponsored by ONT (Gene Remmers), Work Unit 1–2710–197, Project Title "Electric Propulsion," Sub-Task "MHD Propulsion Assessment," Task Area RB23P11, Element 62323N.

INTRODUCTION

HISTORY

Because nuclear reactors use circulating liquid metals as a heat transfer medium, a substantial effort in the past has been devoted to developing liquid metal electromagnetic pumps.[1–3] These pumps, besides being quite reliable, are unusual in their design, since they have essentially no moving parts but the electrical conducting fluid being pumped. The high electrical conductivity of the liquid metals permits pump power efficiencies of nearly 20% under certain conditions.

The direct current, Faraday-type pump is the most elementary electromagnetic pump. The liquid metal is pumped through a duct of rectangular cross section. Two opposite walls of the duct serve as electrodes which, when maintained at an electric potential, cause a high current to flow through the fluid. A strong magnetic induction is passed through the other two walls. Thus, the current direction and the field are mutually perpendicular to each other and perpendicular to the fluid flow in the pump caused by the Lorentz body force.

MHD PROPULSION CONCEPT

In the mid 1960's the electromagnetic pump concept was converted into an overall marine propulsion concept by Stewart Way.[4–7] The basic idea was to pass a current through seawater in the presence of a magnetic induction, in order to accelerate the seawater and to provide a reaction force on the marine vehicle holding the magnet and electrodes. To our knowledge this magnetohydrodynamic (MHD) propulsion concept has not changed significantly since then. The concept can be applied to surface ships and submerged marine vehicles. A number of references are available in the literature on MHD propulsion.[8–17]

MHD PROJECT GOALS

The objectives of the MHD marine propulsion research and development project initiated at the David Taylor Research Center (DTRC) were to examine fundamental principles underlying these MHD propulsion systems and then to produce critical scientific and engineering data and conceptual design information. This program is being coordinated with the Defense Advanced Research Projects Agency (DARPA) MHD Propulsion Program, a cooperative effort with the Naval laboratories, Argonne National Laboratory,

industry, and academia. All the parameters that characterize MHD propulsion systems are to be extensively studied. This approach will establish a baseline group of experimental data and theoretical numerical results to assess the feasibility of marine MHD propulsion for Naval surface ships or submerged vehicles.

It is well known that, in general, MHD propulsion systems have significantly lower propulsive efficiencies than conventional propellers under basically the same propulsion conditions. However, it is generally assumed that these systems will generate much less acoustic noise than propellers, thus making MHD systems more difficult to detect acoustically than conventional propulsion systems. Along with the elimination of rotating seals, gears and shafting, this noise reduction is the major selling point for MHD propulsion systems for Naval propulsion application. Therefore, the principal starting point for this project in fiscal year (FY) 1990 will be to study theoretically the physical principles involved in the generation of acoustic noise in MHD propulsors on submerged vehicles. Little reliable scientific information exists on acoustic signature of these MHD systems.

GOALS OF THIS TECHNICAL REPORT

The MHD propulsion program at DTRC was initiated late in FY89 with a small theoretical effort to investigate MHD propulsion efficiencies, and to develop plans for possible MHD experiments to study acoustic noise in later work. This technical report documents the initial theoretical effort on the MHD program.

A literature search was performed on marine MHD propulsion.[8–17] Since the numerical results in the literature were often too incomplete and sketchy for reliable decision-making, a fundamental set of equations which describe the propulsive efficiencies of an ideal rectangular duct propulsion system was developed into a computer program. Assumptions in the mathematical model were generally made which tend to maximize the propulsive efficiencies of the MHD system. These numerical results can be used for engineering estimates of the propulsive efficiencies of real MHD propulsion systems. The computer program was exercised for a wide variety of cases; the work is described in this report.

This report begins with a background description of fundamental propeller theory. It is shown that the propeller propulsion theory is approximately analogous to a MHD propulsive rectangular duct. Next, the propulsion theory of an MHD rectangular duct was derived from the basic principles of fluid dynamics. From this work, a one-dimensional control volume mathematical model for an ideal rectangular MHD propulsive duct was developed,[18, 19] and the numerical results for propulsive efficiency of different system conditions are presented here in the form of curves and tables.

The MHD propulsion mathematical model will be modified in FY 90 to include channel end effects. The theory of Hughes and McNab[20] was developed for MHD liquid metal pumps and will be applied to MHD seawater propulsion channels. It is expected that these end effects will degrade the propulsive efficiencies calculated for the ideal MHD propulsion model without end effects. End effects are known to have a degrading effect on MHD liquid metal pumps. However, channel duct design in MHD propulsion systems can be used to lessen these end effects.

TRADITIONAL PROPELLER THEORY AND APPROXIMATE EXTENSION TO MHD DUCTS

BACKGROUND

We will begin the discussion with the traditional propeller theory, since this topic closely relates to the understanding of the magnetohydrodynamic (MHD) propulsion problem. The ship being considered is driven at a constant velocity V with a single propeller. The frame of reference is chosen to be moving with the ship. Thus, the fluid unaffected by the propeller has velocity V and pressure P_o. The propeller[21] is simply modelled as a porous disk with area A_D through which water flows. The water flowing through the disk experiences a pressure increase, ΔP, as it passes through the disk representing the propeller. We will designate the pressure on the upstream side of the disk as P_u, which is less than the ambient pressure P_o. Because the relationship $P_u < P_o$ holds, the water is accelerated from V to V_D as it approaches the propeller. Because of this fluid acceleration, the water passing through the propeller comes from a far upstream stream tube with area, A, which is larger than A_D. As the water passes through the disk, its velocity remains V_D, by conservation of mass, but its pressure increases to $(P_u + \Delta P)$, which is greater than the ambient pressure P_o. The high pressure water that leaves the propeller must merge with the surrounding water at P_o, so the water accelerates to the exit velocity V_e, which is greater than the velocity V_D. There is a corresponding reduction in exit area to A_e and a return of the pressure to P_o. In the moving reference frame far downstream of the propeller, we have a jet with elevated velocity V_e and cross–sectional area A_e, surrounded by water with velocity V and pressure at P_o. Figure 1 shows a diagram representing this traditional propeller system.

There are four stations on the diagram. Far upstream at station 1, the ambient pressure is P_o, the area of the free stream tube is A, and the velocity of the fluid is V. At station 2, immediately upstream of the propeller, the pressure P_u is less than the ambient pressure P_o, $P_u < P_o$, the area of the propeller is A_D and the velocity into the propeller is V_D. At station 3, immediately downstream of the propeller, the pressure jumps from P_u immediately upstream to $P_u + \Delta P$ immediately downstream. $P_u + \Delta P$ is greater than the ambient pressure $(P_u + \Delta P) > P_o$, the area of the propeller is A_D, and the velocity coming out of the propeller is V_D. Far downstream the ambient pressure is P_o ; the exit area is A_e, and the exit velocity is V_e.

From conservation of mass the following relationship holds: $VA = V_D A_D = V_e A_e$. The law of conservation of energy can be used to represent the conservation of mechanical energy per unit of mass. This water flowing from a to b along a streamline can be represented by:

$$\frac{P_a}{\varrho} + \frac{V_a^2}{2} + gz_a = \frac{P_b}{\varrho} + \frac{V_b^2}{2} + gz_b + W_s + W_f = Constant\ along\ streamline \quad (1)$$

where:

z = vertical coordinate, with positive direction upward,

$\frac{V^2}{2}$ = kinetic energy per unit mass ,

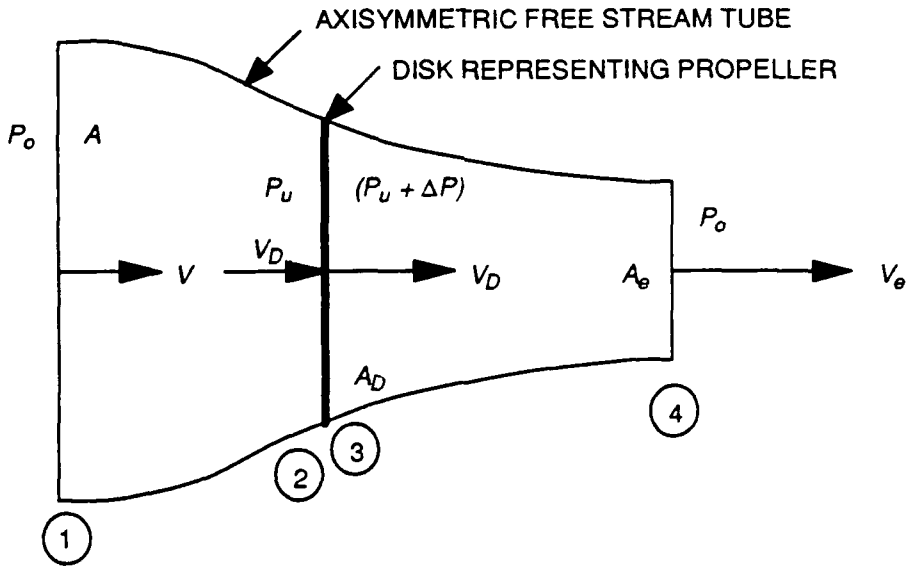

Fig. 1. Stream tube for propeller system.

W_s = work done by fluid per unit mass,
W_f = energy lost to friction flowing from a to b, per unit mass,
gz = potential energy in elevation per unit mass, and
$\frac{P}{\varrho}$ = potential energy in pressure per unit mass.

Like all potential energies, both of these have arbitrary datum, i.e., we can measure all elevations from any horizontal plane and all pressures from any arbitrary constant pressure.

Some authors refer to Eq. 1 as a modified Bernoulli equation. The following assumptions are made in order to simplify Eq. 1:

- Flows are essentially horizontal, and we can subtract out hydrostatic pressure variation, so we ignore the gz terms.
- It is assumed that the propeller is frictionless (not for MHD duct) so that $W_f = 0$ for the propeller case.

Referring to Figure 1 for the diagram for the propeller flow, Eq. 1 from stations 1 to 2 is:

$$\frac{P_o}{\varrho} + \frac{V^2}{2} = \frac{P_u}{\varrho} + \frac{V_D{}^2}{2} \quad , \tag{2}$$

Note that only the propeller does work on fluid (negative W_s). Therefore, $W_s = 0$ from stations 1 to 2, and from stations 3 to 4:

$$\frac{P_u + \Delta P}{\varrho} + \frac{V_D^2}{2} = \frac{P_o}{\varrho} + \frac{V_e^2}{2} \quad , \tag{3}$$

Equation 1 from stations 2 to 3 is:

$$W_s = -\frac{\Delta P}{\varrho} \quad . \tag{4}$$

We will define T here to represent the forward thrust on the propeller disk which is equal to the afterward negative thrust of propeller on water. The thrust from the propeller is:

$$T = (\Delta P)\ A_D \quad . \tag{5}$$

The thrust – T on the submerged vehicle is caused by the reaction force and is equal in magnitude and opposite in direction to the force on the fluid T.

The afterward thrust on the water from the propeller can be calculated from the conservation of linear momentum for steady, incompressible flow through a control volume (that is, a fixed volume in space with control surface). (See Fig. 2.)

$$T = \sum F = \varrho \int\int_{\substack{control \\ surface}} V\, V_n\, dA, \tag{6}$$

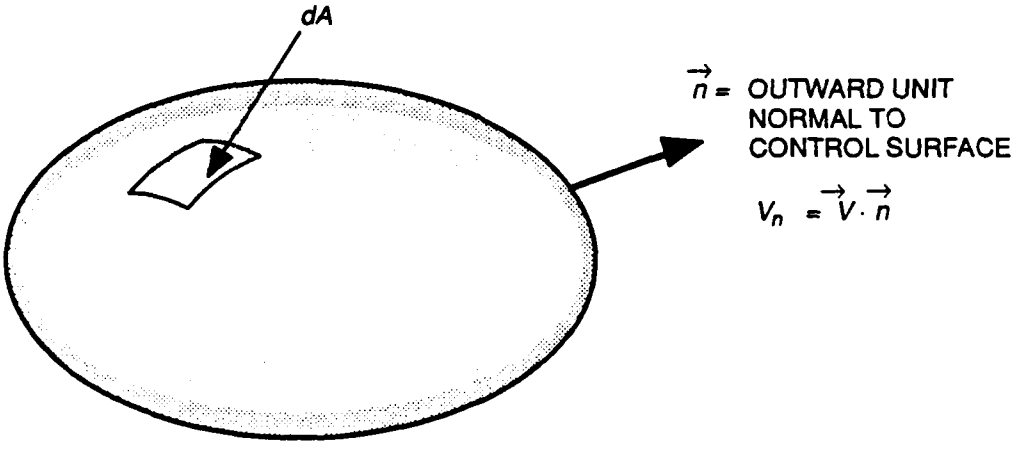

Fig. 2. Control volume in space.

where:

V_n = outward normal component of velocity at a point on control surface ,

dA = differential element of control surface,

$dQ = V_n\, dA$ = volumetric flow across dA per unit time, and

$\sum F$ = sum of all external forces acting on water which is instantaneously inside control surface, including pressure forces from water outside control surface.

Figure 3 shows the control volume for the propeller with the force T acting on the water.

For the control surface for the propeller we assume that $P = P_o$ over entire surface. Therefore, for this problem pressures give zero net force. This is the traditional assumption, which is not strictly true. With this assumption the only external force for the system is the propeller thrust T. At station 1, $V_n = -V$ (fluid inflow) and $V_y = +V$, and the entrance area equals A. At station 4, $V_n = +V_e$ (outward flow of fluid), $V_y = +V_e$, and exit area equals A_e. At the stream tube surface, $V_n = 0$. Substituting these results into Eq. 6 results in the well known expression for the propeller thrust:

$$T = \varrho(V)(-V)A + \varrho(V_e)(V_e)A_e \quad , \tag{7}$$

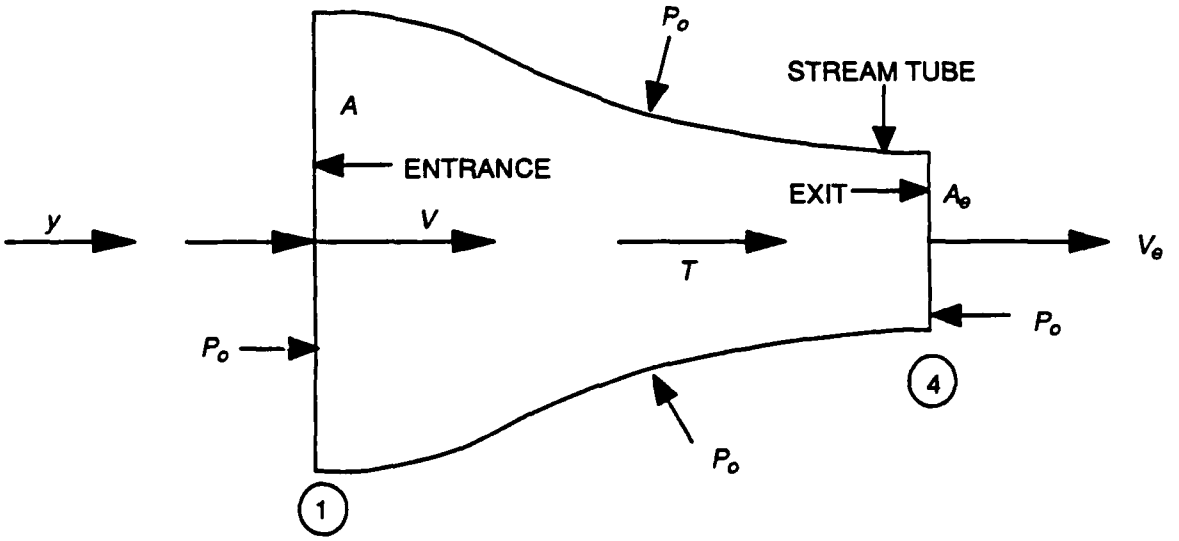

Fig. 3. Control volume for propeller mathematical model.

But from the incompressibility of the water the following relationships holds:

$$Q = VA = V_D A_D = V_e A_e \quad , \tag{8}$$

where Q = volumetric flow rate (m^3/s) . Thus Eq. 7 can be conveniently expressed as:

$$T = \varrho Q(V_e - V) \quad , \tag{9}$$

where Q = mass flow rate (mass per unit time), and $\varrho Q(V_e - V)$ = change in linear momentum per unit time .

First, we consider a traditional manipulation of Eq. 1–9. Then we separate independent from dependent variables in these equations. Equating Eqs. 5 and 9, we obtain:

$$(\Delta P)A_D = \varrho Q(V_e - V) \quad , \tag{10}$$

Since $Q = V_D A_D$, this gives

$$\frac{\Delta P}{\varrho} = V_D(V_e - V) \quad . \tag{11}$$

Subtracting Eq. 2 from Eq. 3:

$$\frac{(\Delta P)}{\varrho} = \frac{1}{2}(V_e^2 - V^2) = \frac{1}{2}(V_e + V)(V_e - V) \quad . \tag{12}$$

Equating Eqs. 11 and 12, we obtain

$$V_D = \frac{1}{2}(V_e + V) \quad . \tag{13}$$

This is a full solution of the energy equation and the momentum equation.

Now consider dependent and independent variables involved in the problem. Take ship velocity V and propeller disk area as the only two independent variables $A_D = (\pi/4)D^2$. The force T, required to move the ship at constant velocity V, is uniquely determined by V and the hull shape. Consider a streamlined submerged vessel with only skin friction drag. Then the following equation holds:

$$Skin\ friction\ drag = T = \frac{1}{2}\varrho V^2 C_f S_W \quad , \tag{14}$$

where:

S_W = wetted surface area of vessel;
C_f = skin friction coefficient, which is a function of Reynold's number; and

$\mathrm{Re}_L = \frac{\varrho V L_V}{\mu}$, where L_v equals vessel length, ϱ equals density of water, and μ equals viscosity of water.

The Reynold's number can be used to determine the skin friction coefficient C_f. If the flow is laminar $(\mathrm{Re}_L < 5 \times 10^5)$ then C_f can be represented by $C_f = \frac{1.33}{(\mathrm{Re}_L)^{1/2}}$. At the transition point where the Reynold's number has the range $5 \times 10^5 < \mathrm{Re}_L < 10^7$, C_f can be represented by $C_f = \frac{0.074}{(\mathrm{Re}_L)^{1/5}} - \frac{1740}{\mathrm{Re}_L}$. In the turbulent region $(\mathrm{Re}_L > 10^7)$, the frictional coefficient C_f can be represented by the Prandtl-Schlichting equation, $C_f = \frac{0.455}{(\log_{10} \mathrm{Re}_L)^{2.58}} - \frac{1700}{\mathrm{Re}_L}$.

Therefore, once we specify V, the required T is known from the skin friction drag, Eq. 14. Since A_D must be specified, the following relationship holds from Eq. 5:

$$\Delta P = \frac{T}{A_D} \tag{15.1}$$

$$\Delta P = \frac{1}{2} \varrho V^2 C_f \left(\frac{S_W}{A_D} \right) . \tag{15.2}$$

Using Eqs. 12 and 15.2, we obtain:

$$V_e = V \left(1 + \frac{C_f S_W}{A_D} \right)^{1/2} . \tag{16}$$

From Eq. 13, V_D is easily obtained:

$$V_D = \frac{V}{2} \left[1 + \left(1 + \frac{C_F S_W}{A_D} \right)^{1/2} \right] . \tag{17}$$

Using the relationship $VA = V_D A_D = V_e A_e$ from the incompressibility of the fluid, we obtain:

$$A = \frac{A_D}{2} \left[1 + \left(1 + \frac{C_f S_W}{A_D} \right)^{1/2} \right] \tag{18.1}$$

$$A_e = \frac{A_D}{2}\left[1 + \left(1 + \frac{C_f\, Sw}{A_D}\right)^{-1/2}\right] . \qquad (18.2)$$

Everything is now determined from V and A_D plus C_f and S_W.

APPROXIMATE RELATIONSHIP OF PROPELLER TO MHD DUCT

We will consider a simple MHD rectangular duct like that of Fig.4. Converging or diverging nozzles attached to a simple duct in general tend to degrade the propulsive efficiency of the duct due to surface friction effects. Therefore, we will discuss a simple rectangular duct in this section, as opposed to a more complicated configuration, because at this point we are interested in the upper limits of propulsive efficiency.

The duct problem is approximately analogous to the traditional propeller problem where the force T is produced by the $\vec{J} \times \vec{B}$ Lorentz body force rather than the propeller force. For a detailed discussion of this analogy, the reader should consult Appendix A.

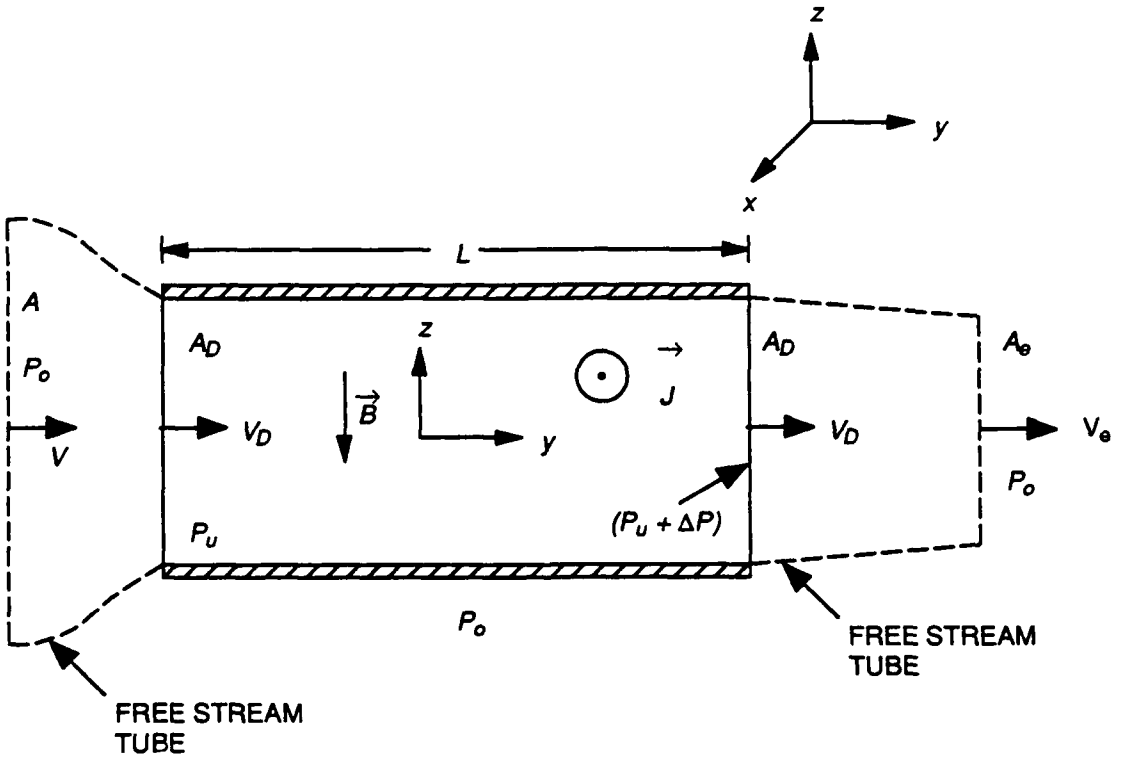

Fig. 4. Simple MHD rectangular duct.

Equations 16, 17, 18.1, and 18.2 give the expressions for V_e, V_D, A and A_e. The duct dimensions are length $L = (\Delta y)$, distance between electrodes $w = (\Delta x)$, distance between insulators $h = (\Delta z)$, and cross sectional area $A_D = wh$. The Cartesian coordinate system (x,y,z) is shown in Fig. 4, where $\hat{x},\hat{y},\hat{z}$ are the unit vectors. Throughout the duct, we ignore end effects. It is well known that duct end effects degrade propulsive efficiency. The velocity of fluid flow in the duct is a constant $V = V_D\hat{y}$, because the duct has a constant cross-sectional area. The electric current density is designated as $\hat{j} = J\hat{x}$, the electric field as $\vec{E} = E\hat{x} = (\phi/w)\hat{x}$, and the voltage difference between electrodes as ϕ. The magnetic field is represented by $\vec{B} = -B\hat{z}$, the Lorentz body force as $\vec{j}x\vec{B} = JB\hat{y}$, and the "back" electromotive force is $\vec{V}x\vec{B} = -V_DB\hat{x}$.

The conservation of energy equation from the entrance to the exit of the duct is $V_{entrance} = V_{exit}, z_{entrance} = z_{exit}$

$$\frac{\Delta P}{\varrho} = -W_s - W_f \ , \tag{19}$$

where:

$-W_s = \dfrac{JBL}{\varrho}$ = work done on a unit mass by electromagnetic body force, $\vec{j}x\vec{B}$, as mass travels from entrance to exit, and

$W_f = \left(\dfrac{fL}{D_h}\right)\left(\dfrac{V_D{}^2}{2}\right)$ = frictional losses per unit mass.

where:

D_h = hydraulic diameter $= \dfrac{4A_D}{Per} = \dfrac{2wh}{(w+h)}$,

Per = perimeter $= 2(w+h)$, and

f = friction factor, which is a function of Re_D, $\dfrac{\epsilon}{D_h}$ and M.

$\mathrm{Re}_D = \dfrac{\varrho V_D D_h}{\mu}$ = Reynold's number based on mean duct velocity and hydraulic diameter, and

ϵ = characteristic wall roughness size, which is considered a property of the wall material. For example, for cast iron the value of ϵ = 0.00085 ft, while for wrought iron, its value is 0.00015 ft.

$\dfrac{\epsilon}{D_h}$ = dimensionless roughness size.

$M = BD_h\left(\frac{\sigma}{\mu}\right)^{1/2}$ = Hartmann number based on hydraulic diameter, and

σ = electrical conductivity of fluid.

Combining Eqs. 15 and 19, we obtain the electric current density required to overcome the frictional resistance in the duct and provide a pressure rise, ΔP, needed to drive the ship at a steady-state condition.

$$J = \frac{\varrho}{2B}\left[\left(\frac{C_f S_W}{A_D}\right)\left(\frac{V^2}{L}\right) + f\left(\frac{{V_D}^2}{D_h}\right)\right] \tag{20}$$

skin friction drag of hull + internal friction of duct flow

The only role of ship length is in the relationship of Re_L to C_f and in S_w. Now we must determine what voltage and power is needed to produce this J.

From the x–component of Ohm's law [22]:

$$J = \sigma\left(\frac{\phi}{w} - V_D B\right) \tag{21.1}$$

$$\text{or} \quad \phi = w\left(\frac{J}{\sigma} + V_D B\right) \quad . \tag{21.2}$$

Equation 21 gives the voltage difference between plates required for this thrust. The propulsive efficiency η is represented by the relationship:

$$\eta = \frac{TV}{\phi I} \quad . \tag{22}$$

T is given by Eq. 5 and ϕ is given by Eq. 21.2, in terms of J and V_D. The total current across the rectangular channel is $I = JhL$.

MATHEMATICAL MODEL OF MAGNETOHYDRODYNAMIC (MHD) SHIP PROPULSION WITH PROPULSIVE EFFICIENCY

FUNDAMENTAL EQUATIONS OF MHD PROPULSION

This section presents the development of the fundamental equations for an MHD propulsive rectangular duct on a submerged vehicle. The duct configuration under consideration is presented in Fig. 5. The fluid flow into, through, and out of the duct is represented by a stream tube of total surface area $\Sigma = \Sigma_1 + \Sigma_2 + \Sigma_3 + A + A_e$ and total volume $V' = V_1' + V_2' + V_3'$. The duct together with the stream tube is surrounded by an ambient pressure P_o. The duct is of uniform cross-sectional area A_D. The entrance area and exit area of the stream tube are A and A_e respectively. The pressure at the entrance of the stream tube is P_o, at the duct entrance P_u, at the duct exit $P_u + \Delta P$, and at the stream tube exit P_o. The following inequalities hold for the pressures: $P_o > P_u$, $P_u < P_u + \Delta P$, and $P_u + \Delta P > P_o$. The velocity of the fluid entering the stream tube is V, entering the duct V_D, leaving the duct V_D, and leaving the stream tube V_e. The unit normal to the stream tube $\vec{n}$ is outward from the surface.

The Cartesian coordinate system (x, y, z) has the origin fixed in the center of the duct and moves with the duct at constant velocity V. The observer is therefore considered to be travelling with the duct. The constant, homogeneous magnetic induction $\vec{B}$ is in the negative z–direction. The constant, homogeneous current density vector lines are in the positive x–direction. The fluid flows in the positive y–direction.

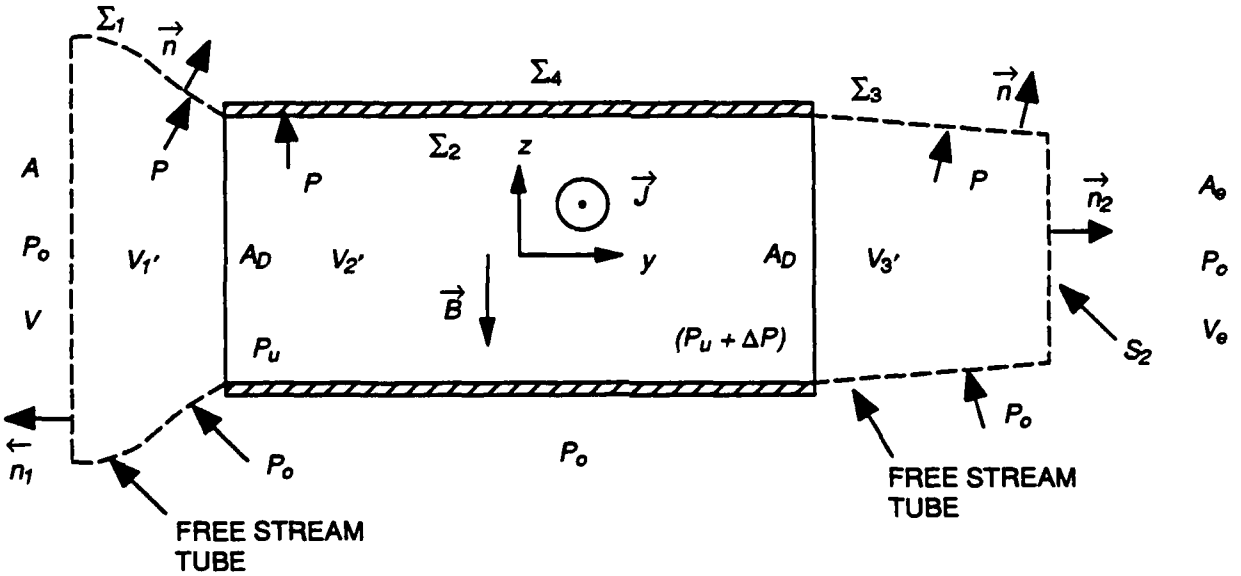

$$\Sigma = A + A_e + \Sigma_1 + \Sigma_2 + \Sigma_3$$

$$V' = V_1' + V_2' + V_3'$$

Fig. 5. MHD rectangular duct.

Using the above rectangular duct configuration, we shall develop the general fundamental equations for deriving the propulsive efficiency of the rectangular MHD duct in a steady state condition. The following fundamental principles from theoretical physics for fluid flow will be used for the derivation.

- Conversation of linear momentum for a stationary control volume
- Rate of change of kinetic energy for a stationary control volume (Energy Theorem)
- The principle of action and reaction
- Ohm's law for electrical conductors

This derivation implies the conservation of mass, linear momentum, energy, and angular momentum for the system.

Also, the approximations to these equations are developed for the mathematical model that was used to produce the numerical computer results presented in the report. This development follows well-known concepts of fluid mechanics for fluid flow through a stationary control volume and is discussed in detail to clarify the concepts involved in an MHD duct.

Conservation of Linear Momentum

Newton's Second Law states that the sum of all external forces acting on an assemblage of masses equals the rate of change of the total linear momentum of the assemblage. Our assemblage is the mass of fluid instantaneously inside the control volume V' in Fig. 5. Since fluid is continuously entering and leaving our fixed control volume, there are two different assemblages of masses at two different times. A change of the linear momentum of the assemblage instantaneously inside the control volume appears in two forms. First, the velocity at points inside the control volume may be increasing or decreasing with time, so that the assemblage of masses inside the control volume at time $(t+dt)$ has more or less linear momentum than the assemblage at t. These two assemblages differ only by the control surface, $\Sigma = A + A_e + \Sigma_1 + \Sigma_2 + \Sigma_3$, during the short interval from t to $(t+dt)$. This first change of linear momentum is given by

$$\frac{\partial}{\partial t}\int_{V'} \varrho V_i dV', \tag{23.1}$$

where V_i are the components of the velocity $\vec{V}$, and dV' is a differential volume element. The second realization of a linear momentum change is that the fluid leaving the control volume may have more or less linear momentum that the fluid entering it. This second change of linear momentum is given by

$$\int_{\Sigma} \varrho V_i V_k n_k \, dS, \tag{23.2}$$

where n_k are the components of the outward unit normal $\vec{n}$ at each differential element dS of the control surface S. The volume of fluid crossing the element dS of the control surface per unit time is $V_k\, n_k\, dS$, which is positive or negative for fluid leaving or entering, respectively, while the linear momentum of this fluid per unit volume is ϱV_i. Therefore, Newton's Second Law for a Control Volume, which is an Open System, is

$$\sum F_i = \frac{\partial}{\partial t}\int_{V'} \varrho\, V_i dV' + \int_{\Sigma} \varrho\, V_i V_k n_k\, dS \quad , \tag{24}$$

where $\sum F_i$ is the sum of all external forces acting on the mass instantaneously inside the control volume. The sum of forces is given by

$$\sum F_i = \int_{V'} b_i\, dV' + \int_{\Sigma} t_i\, dS \quad , \tag{25.1}$$

where b_i is the external body force per unit volume at each point inside the control volume, and t_i is the external traction force per unit area at each point on the control surface. For a viscous fluid

$$t_i = -Pn_i + \sigma_{ik}'\, n_k \quad , \tag{25.2}$$

where P is the pressure and σ_{ik}' is the viscous shear stress.[23] If P represents the deviation of the actual pressure from the hydrostatic pressure, than we can ignore the gravitational body force, so that our only body force is the Lorentz force per unit volume,

$$b_i = \epsilon_{ijk}\, J_j B_k \quad , \tag{25.3}$$

where ϵ_{ijk} is the permutation tensor, J_j is the electric current density, and B_k is the magnetic induction. We consider a steady flow, so that the velocity at each point inside the control volume is independent of time, and Newton's Second Law is

$$\int_{\Sigma} \varrho V_i V_k n_k\, dS = \int_{V'} \epsilon_{ijk} J_j B_k\, dV' + \int_{\Sigma} \sigma_{ik}' n_k\, dS - \int P n_i\, dS \quad . \tag{26}$$

The sum of the external forces on the right-hand side act on the seawater which is inside the control surface S. The first term is the total Lorentz body force on the fluid in the rectangular channel plus end effects. The second term represents the frictional forces of the fluid along the surfaces $\Sigma_1 + \Sigma_2 + \Sigma_3$. The frictional force along the inside walls of the duct Σ_2 is more important than the frictional force along $\Sigma_1 + \Sigma_3$. The third term includes the pressure forces from the fluid external to the control surface. The following integrals can be evaluated in Eq. 26.

$$\int_{\Sigma} \varrho V_i V_k n_k \, dS = \varrho Q (V_e - V) \hat{\underline{x}} \tag{27.1}$$

where $Q = VA = V_D A_D = V_e A_e$.

$$\int P \vec{n} \, dS \cong 0 \tag{27.2}$$

$$\int_{\Sigma} \sigma_{ik}' n_k \, dS \cong \int_{\Sigma_2} \sigma_{ik}' n_k \, dS \tag{27.3}$$

Substituting these integrals in Eq. 26 results in the following equation:

$$\varrho Q (V_e - V) \hat{\underline{x}} = \int_{V'} (\vec{J} \times \vec{B}) dV' + \int_{\Sigma_2} \sigma_{ik}' n_k \, dS \quad . \tag{28.1}$$

For the interior surface of the duct Σ_2,

$$\sigma_{ik}' n_k = -\tau_w \hat{\underline{x}} = -\frac{1}{8} f \varrho V_D^2 \hat{\underline{x}} \quad , \tag{28.2}$$

where τ_w is the viscous wall shear stress and f is the Moody friction factor. If we ignore all electromagnetic end effects, the x–component of Eq. 28.1 is

$$\varrho Q (V_e - V) = JBV_2' - \frac{1}{8} f \varrho \, V_D^2 L \, (Per) \tag{28.3}$$

$$T = Lorentz\ force - Internal\ Friction\ force$$

$$V_2' = LWh$$

where L, W, h, V_2', and $(Per) = 2(w+h)$ are the length, width, height, interior volume, and cross sectional perimeter, respectively. Equation 28.3 is also obtained by substituting Eq. 19 into Eq. 10. The term T is designated as the effective thrust on the fluid down the channel. Equation 28.3 is the fundamental momentum equation for the operation of the MHD duct.

Principle of Action and Reaction

The reaction force–T to the effective Lorentz body force T propels the submerged vehicle at a steady state velocity $\vec{V}$ in the fluid. The reaction force–T balances the hydrodynamic resistance R of the vehicle. The reaction force–T is caused by the magnetic

induction $\vec{B}$ from the current density in the channel interacting with the current in the channel magnetic coil electrical system. Therefore, the useful power in propelling the submerged vehicle by the MHD duct is expressed as

$$\textit{Useful power in propelling vehicle} = TV \tag{29}$$

The reaction to the force JBV_2' acts directly on the MHD channel magnets.

For a more detailed discussion of the reaction force see Appendix A.

Rate of Change of Kinetic Energy (Energy Theorem)

The dot product between Newton's Second Law for a single mass and the mass's velocity vector gives an equality between the rate of change of the mass's kinetic energy and the work done on it per unit time. When we sum the Newton's Second Law for an assemblage of masses, all internal forces between the masses sum to zero, since the forces between two masses are equal and opposite. When we sum the kinetic energy equation for an assemblage of masses, the work done by the internal forces does not sum to zero. In a continuum model, the internal forces are represented by the pressure and viscous stresses. The pressure force is conservative for a liquid, so it can only transfer kinetic energy between masses with no net change in the total kinetic energy of the assemblage. The viscous stresses are not conservative and produce an irreversible conversion of kinetic energy to heat. The rate of energy conversion per unit volume is called the viscous dissipation Φ and is proportional to the product of the viscous stress between neighboring masses and their *difference* in velocity, as reflected in the velocity gradient,

$$\dot{\Phi} = \sigma_{ik}' \frac{\partial V_i}{\partial x_k} = \textit{viscous dissipation.} \tag{30}$$

The rate of change of the kinetic energy of the assemblage of masses instantaneously inside the control volume is equal to the rate of increase of kinetic energy inside the control volume, plus the difference between the kinetic energies in the fluid entering and leaving the control volume. Thus, the rate of change of kinetic energy for a control volume is

$$\frac{\partial}{\partial t}\int_{V'} (1/2)\varrho V^2 dV' + \int_{\Sigma} (1/2)\varrho V^2 V_k \, n_k \, dS$$
$$= \int_{V'} (b_i V_i) \, dV' + \int_{\Sigma} t_i V_i \, dS - \int_{V'} \sigma_{ik}' \frac{\partial V_i}{\partial x_k} dV' \, , \tag{31}$$

where again b_i and t_i represent the external body force and surface traction.

Alternatively, we can begin with the First Law of Thermodynamics, which states that the heat added to an assemblage of masses, plus the work done by the external forces, equals the change in total energy, which is the sum of the kinetic and internal energies. The internal energy represents the internal energy of the molecular states. We can split the First Law of Thermodynamics into two separate equations, with the heat and work in the internal and kinetic energy equations, respectively. In making this split, we must add

equal and opposite source terms to each equation to represent the energy transfer between internal and kinetic energies. In a gas, internal energy can be converted to kinetic energy through volumetric expansion, but in a liquid, the only energy transfer is the viscous conversion of kinetic energy to internal energy. After the split of the First Law, the kinetic energy equation is Eq. 31.

Introducing Expressions 25.2 and 25.3, where again P represents the deviation from hydrostatic pressure, Eq. 31 becomes

$$\frac{\partial}{\partial t}\int_{V'}(1/2)\varrho V^2 dV' + \int_{\Sigma}[(1/2)\varrho V^2 + P]\ V_k n_k\ dS$$

$$= \int_{V'}\left(V_i \epsilon_{ijk} J_j B_k\right)\ dV' + \int_{\Sigma}\sigma_{ik}' V_i\ n_k\ dS - \int_{V'}\sigma_{ik}'\frac{\partial V_i}{\partial x_k}\ dV' \ . \qquad (32)$$

Our flow is steady, so that the first term in Eq. 32 is always zero. We can apply Eq. 32 separately to the smaller control volume V_1' or V_3' in Fig. 5. We are neglecting viscous stresses in these volumes, and $\vec{J} \times \vec{B} = 0$ here since we neglect electromagnetic end effects. Therefore, Eq. 32 becomes

$$Q[(1/2)\varrho V_D^2 + P_\mu - (1/2)\varrho V^2 - P_o] = 0 \qquad (33.1)$$

$$Q[(1/2)\varrho V_e^2 + P_o - (1/2)\varrho V_D^2 - P_\mu - \Delta P] = 0 \qquad (33.2)$$

for volumes V_1' and V_3', respectively. The Eqs. 33.1 and 33.2 are identical to the conservation of energy equations (Eqs. 2 and 3) after dividing through by Q. When we apply Eq. 32 to the other smaller control volume V_2' in Fig. 5, we must determine the two viscous terms on the right-hand side. We use a one-dimensional flow model with $\vec{V} = V_D \hat{x}$ throughout V_2'. Therefore, $\frac{\partial V_i}{\partial x_k} \equiv 0$, and the viscous work is the work done by the fluid moving at velocity $V_D\hat{x}$ against the viscous wall shear stress, $-\tau_w \hat{x}$ at Σ_2, which contributes

$$-\tau_w V_D L(Per) = -\frac{1}{8} f \varrho V_D^3 L(Per) \qquad (34)$$

to the right side of Eq. 32. In reality, the fluid at Σ_2 must be at rest, so that $\sigma_{ik}' V_i n_k = 0$ at Σ_2, and it is the final viscous dissipation term which represents the work done against viscous forces. Actually, this distinction is moot because the Moody friction factor is defined by equating the Expression 34 to the power input needed to maintain a constant kinetic energy in spite of frictional losses. For the control volume for V_2', Eq. 32 becomes

$$Q(\Delta P) = V_D JBV_2' - \frac{1}{8} f\varrho V_D{}^3 L(Per) \quad . \tag{35}$$

If we divide this equation by $\varrho Q = \varrho V_D A_D$, it becomes Eq. 19.

Electromagnetic Energy Input

In our frame of reference moving with the duct, there is an electric filed $\vec{E}$, a magnetic induction $\vec{B}$, and an electric current density $\vec{J}$ in the fluid with electrical conductivity σ inside our control volume. The electromagnetic energy input to the fluid per unit time is[24]:

$$\int_{V'} \left(\vec{J} \cdot \vec{E}\right) dV' \quad . \tag{36}$$

If we introduce Ohm's law without Hall effects,

$$\vec{J} = \sigma \left(\vec{E} + \vec{V} \times \vec{B}\right) \quad , \tag{37}$$

in order to eliminate $\vec{E}$, then Expression 36 becomes

$$\int_{V'} (J^2/\sigma)\, dV' + \int_{V'} \vec{V} \cdot \left(\vec{J} \times \vec{B}\right) dV' \quad . \tag{38}$$

The second term in Eq. 38 is the work done on the fluid by the Lorentz body force (Eq. 25.3), and this term appears in our kinetic energy equation (Eq. 32). The first term in Eq. 38 represents a heat input because an electric current flowing in a conductor produces heat. This heat input is called the Joulean heating and appears as a term in the conservation of internal energy equation, along with the viscous dissipation (Eq. 30) as two volumetric heat sources. Since we cannot get any useful work out of the internal energy of a liquid, the Joulean heating represents an energy loss for our system. Equation 36 represents the total electrical power input to the MHD system and is equal to

$$JEV_2' = I\phi = V_D JBV_2' + I^2 R_e \quad , \tag{39}$$

where $I = JLh$ = the total current between the electrodes, $\phi = Ew$ = total voltage difference between electrodes, h = height between insulating walls, w = width between electrodes, and $R_e = (w/\sigma Lh)$ is the electrical resistance of the duct.

Efficiencies For MHD Propulsion

The basic propulsion equations for the MHD rectangular duct were derived and presented previously in the report. We assume that the following quantities are known:

V = velocity of the vessel;
C_f = skin friction coefficient of the vessel;
S_w = wetted surface area of the vessel;
L, w, h = length, width and height of MHD propulsion duct;
B = strength of uniform magnetic induction inside duct.

Other quantities are given by the following equations:

T = skin friction drag resistance of vessel which equals thrust developed by propulsion unit, from Eq. 14;
ΔP = pressure rise through the duct, from Eq. 15;
V_e = exit velocity from control volume, from Eq. 16;
V_D = velocity inside duct, from Eq. 17;
A = area at the entrance of the control volume, from Eq. 18.1;
A_e = area at the exit of the control volume, from Eq. 18.2;
J = uniform electric current density between electrodes inside duct, from Eq. 20;
ϕ = total voltage difference between electrodes, from Eq. 21.2;
η = propulsive efficiency, from Eq. 22.

For the purposes of interpretation, we can split the propulsive efficiency into three separate efficiencies,

$$\eta = \frac{TV}{\phi I} = \eta_e \eta_t \eta_d \quad . \tag{40.1}$$

The electrical efficiency

$$\eta_e = \frac{V_D\, JBLwh}{\phi I} = 1 - \frac{I^2 R_e}{\phi I} \tag{40.2}$$

is the ratio of the work done by the Lorentz force on fluid per unit time to the total electrical power input to duct. Equation 39 has been substituted in order to get the second expression, which shows that $(1-\eta_e)$ is the fraction of the electrical input power which is lost to Joulean heating. The thrust efficiency

$$\eta_t = \frac{TV_D}{V_D JBLwh} = 1 - \frac{(1/8) f \varrho V_D^3 L(Per)}{V_D JBLwh} \tag{40.3}$$

is the ratio of the energy gained by the fluid per unit time inside the duct to the work done by the Lorentz force per unit time. Equation 28.3 has been substituted in order to obtain the second expression, which shows that $(1-\eta_t)$ is the fraction of the work done by the Lorentz force which is lost to the internal friction of the duct. The hydraulic efficiency

$$\eta_d = \frac{TV}{TV_D} = 1 - \frac{(1/2)\varrho Q(V_e - V)^2}{TV_D} \qquad (40.4)$$

is the ratio of the power driving the vessel to the energy gained by the fluid inside the duct per unit time. Equations 9 and 13 were substituted to obtain the second expression. In a fixed frame of reference, the water entering our control volume has zero velocity, while that leaving has a velocity $(V_e - V)$. The kinetic energy in the stream of the duct represents a loss of energy per unit time, which is $(1/2)\varrho Q(V_e - V)^2$.

Up to this point we have implicitly assumed that the MHD propulsion duct is inside the vessel's hull, so that the only skin friction drag resistance is that of the hull. If the duct is housed in an external pod which is connected by a strut to the hull, then the thrust delivered to the hull is reduced by the skin friction drag on the pod and strut. Thus, Eq. 28.3 must be replaced by

$$T = JBLwh - (1/8)f\varrho V_D^2 L(Per) - (1/2)\varrho V^2 C_{fp} S_p \ , \qquad (41)$$

where T is the thrust delivered to the hull, which balances the skin friction drag of the hull, as given by Eq. 14, C_{fp} is the skin friction coefficient for the pod and strut, and S_p is the wetted surface area of the pod and strut. Then Eq. 20 is replaced by

$$J = \frac{T}{BLwh} + \frac{\varrho}{2B}\left[\frac{f}{D_h} V_D^2 + \frac{C_{fp} S_p}{Lwh} V^2\right] \ . \qquad (42)$$

As a conservative estimate of the pod's skin friction drag, we use

$$C_{fp} = 0.075\left[\log_{10}\left(\frac{\varrho VL}{\mu}\right) - 2\right]^{-2} + 0.0005 \ , \qquad (43.1)$$

$$S_p = L(Per) \ , \qquad (43.2)$$

where C_{fp} is given by a variation of the Schoenherr equation which applies for $0.0026 \le C_{fp} \le 0.0037$. Of course, S_p must be much larger than $L(Per)$ because the pod must contain the large magnets needed to produce B. Therefore, Eq. 42 becomes

$$J = \frac{T}{BLwh} + \frac{\varrho}{2BD_h}\left(fV_D^2 + 4C_{fp}V^2\right) \ . \qquad (44)$$

In addition, Eq. 17 is replaced by

$$V_D = \frac{V}{2}\left[1 + \left(1 + \frac{2T}{\varrho A_D V^2} + \frac{4C_{fp}L}{D_h}\right)^{1/2}\right] . \tag{45}$$

Equations 21.2, 44, and 45 now give ϕ, and Eq. 22 gives the propulsive efficiency. Rather than apply this analysis to specific submerged vessels, we will replace Eq. 14 by

$$T = KV^2 , \tag{46}$$

with K = 1000, 2000, 3000, 4000 or 5000 kg/m for some typical submerged vessels. If the MHD propulsion duct is in an external pod, then we use Eqs. 21.2, 43.1, 44, 45, and 46 to compute the propulsive efficiency which we denote by η_2. If the duct is inside the vessel's hull, we use the same equations with $C_{fp} = 0$ and denote the propulsive efficiency by η_1.

Numerical Results

The objective at this point of the work was to calculate the propulsive efficiencies η_1 and η_2 of the one-dimensional control volume MHD system at different steady state conditions. These numerical curves presented herein will determine the approximate upper limits of the MHD propulsive vehicular system efficiencies, which can be used for engineering judgments in estimating the propulsive efficiencies under different conditions of "real world" systems used on submerged vehicles. The efficiency is defined as the useful power to propel the vehicle divided by the total electrical power to the duct $I\phi$, where I is the total current across the duct and ϕ is the voltage drop across the duct. * For the efficiency η_1 the useful power to propel the duct is defined mathematically as the ideal thrust in the duct multiplied by the vehicular speed V minus the frictional force in the duct $(1/8)[f\varrho V_D^2 L(Per)]$ multiplied by V. The efficiency η_2 corresponds to an MHD duct in the form of a pod attached by struts to the vehicle hull. The propulsive efficiency η_2 is defined analogously to the propulsive efficiency η_1. In this case, the useful power to propel the submerged vehicle is the ideal thrust in the duct multiplied by V minus both the frictional force in the duct due to fluid flow $(1/8)[f\varrho V_D^2 L(Per)]$ and the force due to the fluid flow outside the pod $(1/2)[\varrho V^2 L(Per)C_{fp}]$, where both frictional terms are multiplied by V. From these definitions $\eta_1 > \eta_2$ under the same propulsion conditions.

The MHD propulsive mathematical model using equations from the previous section were programmed on the computer. All equations are in the SI system of units. The MHD rectangular duct system was considered to be propelling a submerged vehicle at a steady-state condition V. Transient conditions were not considered at this point of the

* Note that this number does not account for power generation or distribution efficiencies.

work. End effects, bubble generation power losses, and the effects of bubbles in the duct were also omitted. Computer calculations were performed using various input parameters for the rectangular duct and various hydrodynamic resistances for the submerged vehicle.

To properly characterize the MHD propulsive system propelling a submerged vehicle of hydrodynamic resistance 3,000 V^2 newtons, we present the base line numerical numbers in Table 1. We consider a rectangular duct height h of 4 meters, width w of 4 meters, and length L of 10 meters (see Fig. 6). A realistic magnetic induction B of 6 tesla across the duct was chosen. The electrical conductivity σ and density of seawater ϱ were chosen to be 4 siemens/m and 1026 kg/m^3, respectively. The remainder of the calculated data with dimensional units is shown in Table 1. The Moody friction factor f (i.e., $f = (4C_{fd})$ for inside the MHD duct corresponds approximately to that for smooth pipes for all numerical results in this report.

Figure 7 presents the total power consumption of the vehicular system versus vehicle speed V. The propulsive efficiency η_1 was used in this plot. The solid curve

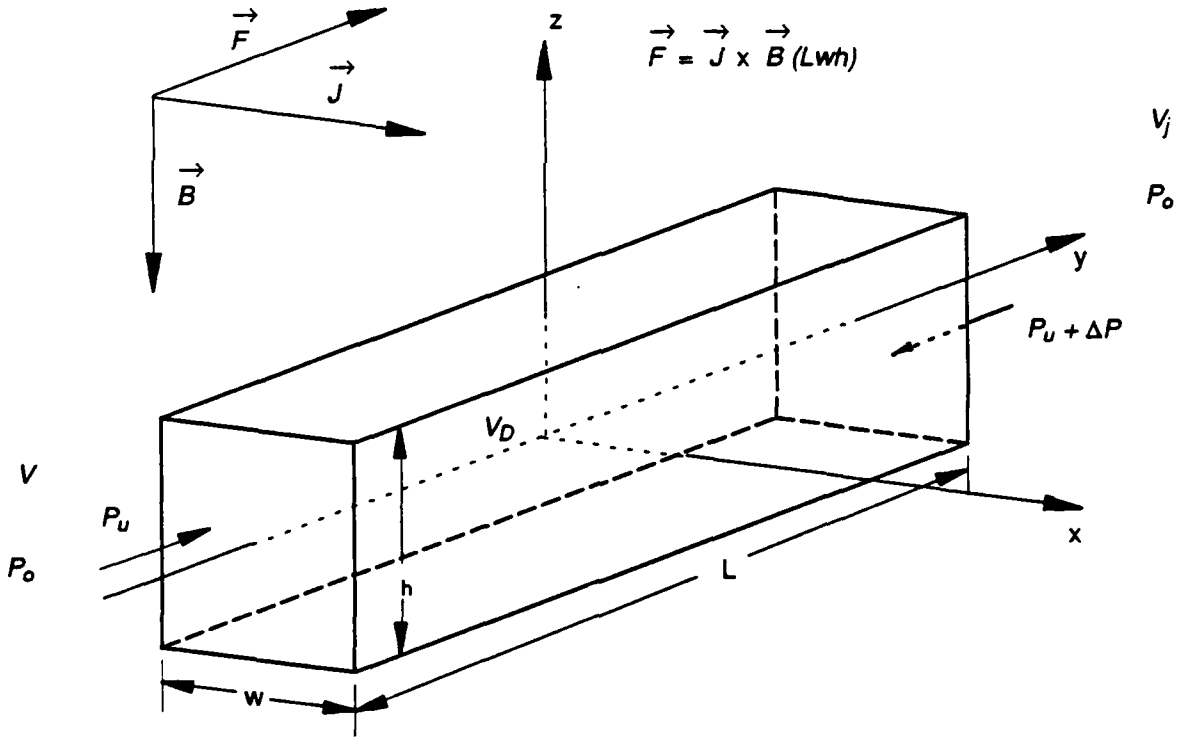

Fig. 6. Propulsive magnetohydrodynamic rectangular duct configuration.

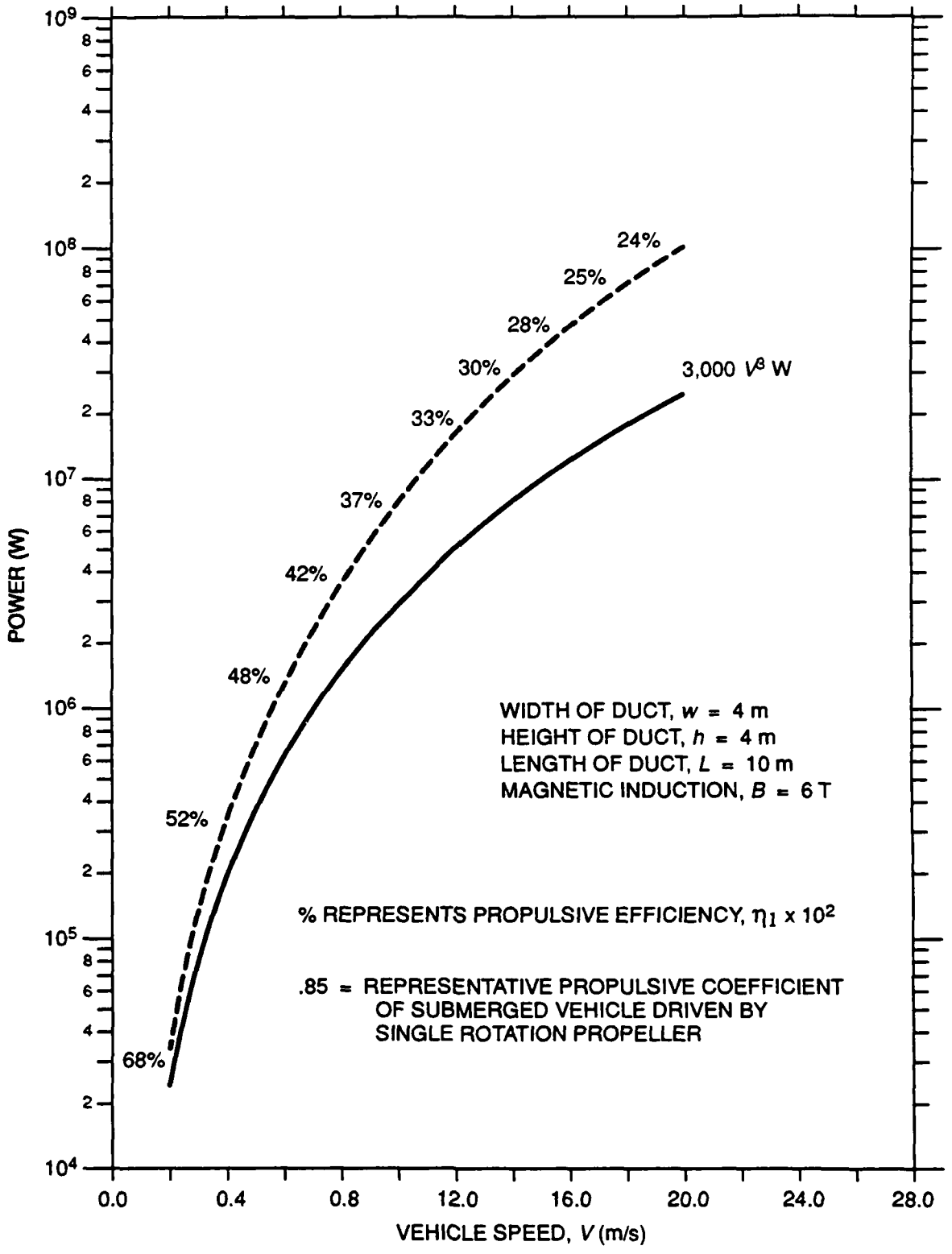

Fig. 7. Power consumption versus submerged vehicle speed.

Table 1. Baseline numerical results for square rectangular duct.

Height of square duct, h	4 meters	Joulean heat loss in duct, I^2R	4.59×10^6 watts
Width of square duct , w	4 meters	Electrical current in duct, I	1.36×10^4 amperes
Length of square duct L	10 meters	Coefficient of skin friction outside in duct, C_{fd}	0.00262
Magnetic induction of duct, B	6 tesla	Coefficient of skin friction outside of duct, C_f	0.002637
Velocity of vehicle, V	10 meters/second	Total input power to propulsive system	8.12×10^6 watts
Velocity of fluid in duct, V_D	10.8 meters/second	Propulsive efficiency, η_1	0.37
Viscosity of seawater, η'	10^3 newton-seconds/meter	Useful power to propel vehicle	3.0×10^6 watts
Electrical conductivity of seawater	4.0 siemens/meter	Power to overcome skin friction of duct	0.28×10^6 watts
Density of seawater, ϱ	1026 kilograms/meter^3	Power to overcome external skin friction	0.0000
Electrical potential across electrodes	599.0 volts	Power lost to kinetic energy aft	0.25×10^6 watts
Electrical resistance of duct, R_e	0.025 ohms	Hydrodynamic resistance of vehicle	3.0×10^5 newtons
Electrical current density, J	338.9 amperes/meter^2		

Nondimensional parameters of duct based on hydraulic diameter, D_h
(Transverse dimension related to fully developed fluid flow)

Reynold's number $$\mathrm{Re}_D = \frac{\varrho V_D D_h}{\eta'} = 44.3 \times 10^6 = \frac{\textit{inertial force}}{\textit{viscous force}}$$

Magnetic Reynold's number $$\mathrm{Re}_m = V_D D_h \sigma\mu = 21.7 \times 10^{-5} = \frac{\textit{induced magnetic induction}}{\textit{external magnetic induction}}$$

Interaction number $$N_D = \frac{\sigma B^2 D_h}{\varrho V_D} = 5.2 \times 10^{-2} = \frac{\textit{pondermotive force}}{\textit{inertial force}}$$

Hartmann number $$M_D = LB\left(\frac{\sigma}{\eta'}\right)^{1/2} = 3.8 \times 10^3 = \frac{\textit{pondermotive force}}{\textit{viscous force}}$$

Nondimensional parameters of duct based on length, L
(Axial dimension related to boundary growth at entrance of channel)

$$\mathrm{Re}_L = \frac{\varrho V_D L}{\eta'} = 110.8 \times 10^6 \qquad N_L = \frac{\sigma B^2 L}{\varrho V_D} = 13 \times 10^{-2}$$

$$\mathrm{Re}_{mL} = V_D L \sigma\mu = 54.3 \times 10^{-5} \qquad M_L = LB\left(\frac{\sigma}{\eta'}\right)^{1/2} = 9.5 \times 10^3$$

presents the power in watts required to propel the submerged vehicle at constant speed. The dimensions of the duct are the same as in Table 1. The magnetic induction B was 6 tesla. The dotted line shows the total input power required to propel the vehicle system. The percentages above the dotted line show the propulsive efficiency η_1. It should be carefully noted that a representative propulsive efficiency of a submerged vehicle driven by a single screw rotation propeller could be considered to be about 85%. These curves show clearly that the propulsive efficiency of this MHD system decreases significantly with vehicle speed V, and that the propulsive efficiency is much less than that of a propeller.

Figure 8 presents the propulsive efficiency curves η_1 and η_2 of a square MHD propulsive duct with a 6 tesla magnetic induction B across the duct, propelling a submerged vehicle at a steady state speed V. The duct has the same linear dimensions as the duct in the previous figure. The hydrodynamic resistance of the vehicle was again 3,000 V^2 newtons and the power required to propel the vehicle is thus 3000 V^3 watts. The propulsive efficiency $\eta_1 > \eta_2$, as would be expected because η_2 incorporates the loss of

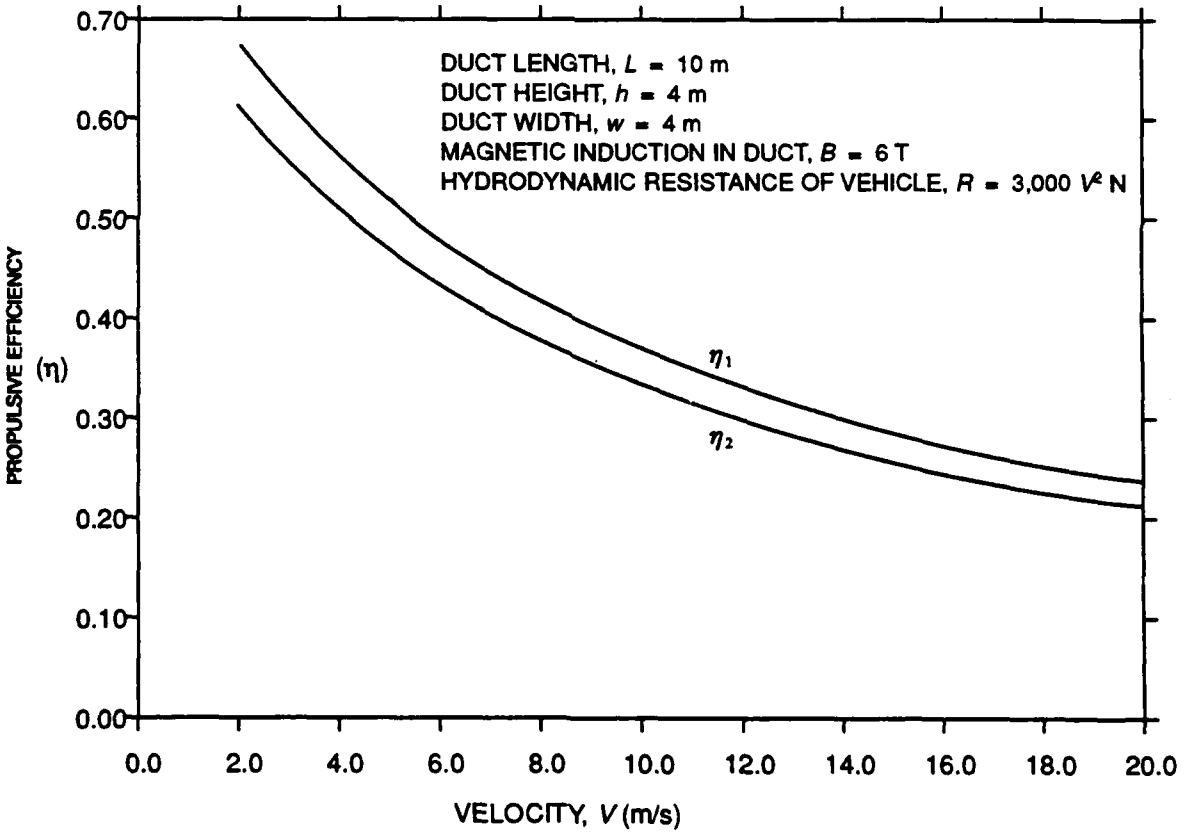

Fig. 8. Propulsive efficiency of square MHD duct versus vehicle speed in meters per second.

power due to the flow of fluid over the external surface of the duct. This corresponds to the duct as a pod attached to the vehicle. Both curves of propulsive efficiency η_1 and η_2 show a significant decrease in propulsive efficiency with speed V.

Figure 9 presents the effective thrust T in newtons versus vehicle speed V in meters per second required to propel a submerged vehicle with a hydrodynamic resistance in seawater of order 3,000 V^2 newtons. The thrust curve is proportional to V^2 and thus rises steeply with V. One knot is equal to 0.5144 m/second.

Figure 10 presents the propulsive efficiencies η_1 and η_2 of the previously described propulsive MHD duct versus constant, homogeneous magnetic induction B across the duct at vehicular speed V of 10 m/second. Using state-of-the-art superconducting magnets, a magnetic induction of 6 to 10 tesla in a large volume is probably the highest magnetic induction that could be obtained in practice. The 6 and 10 tesla limits are shown by two vertical dotted lines on the figure. The propulsive efficiencies η_1 and η_2 increase significantly with the magnitude of the magnetic induction B. The power to propel the vehicle T is 3000 V^3 watts. The magnitude of the separation between η_1 and η_2, $|\eta_1 - \eta_2|$, increases with increasing B.

Figure 11 presents the propulsive efficiencies of the MHD propulsive duct at a vehicular speed of 10 m/second versus electrical fluid conductivity σ in a 6 tesla magnetic induction B. The propulsive efficiencies η_1 and η_2 increase significantly with fluid electrical conductivity σ in siemens per meter. The propulsive efficiencies of the MHD system in the seawater at the polar ice caps (i.e. $\sigma = 0.4$ siemens/m) is well below an efficiency of 0.10 for either η_1 *or* η_2. The hydrodynamic resistance of the submerged vehicle was again 3000 V^2 newtons.

Figure 12 presents the propulsive efficiencies of a MHD propulsive duct of length L equal to 10 m and varying square cross-sectional area from 4 m^2 to approximately 81 m^2. The variation of cross-sectional area is shown in the horizontal axis. The magnetic induction across the duct is 6 tesla, and the power required to propel the submerged vehicle is 3000 V^3 watts. The efficiencies η_1 and η_2 increase significantly with increasing cross-sectional duct area. The magnitude of separation $|\eta_1 - \eta_2|$ between η_1 and η_2 becomes significant at large duct cross-sectional areas. It should be realized that construction of superconducting magnets for a duct with width w and height h much greater than 4 m would probably be impossible with present technology.

Figure 13 presents the propulsive efficiencies of a duct of width w of 4 m and a height h of 4 m with a varying length L in meters at a vehicular speed of 10 m/second. The efficiencies η_1 and η_2 increase slowly with duct length L in meters. The magnetic induction across the duct B is 6 tesla. The maximum duct length considered in this figure is 20.0 m.

Figures 14 through 18 show the effect of changing the MHD rectangular duct width w through the values 1, 2, 4, 8, and 16 m on the duct propulsive efficiencies η_1. On each figure for a specific duct of width w the value of the duct height h is increased from 4 to

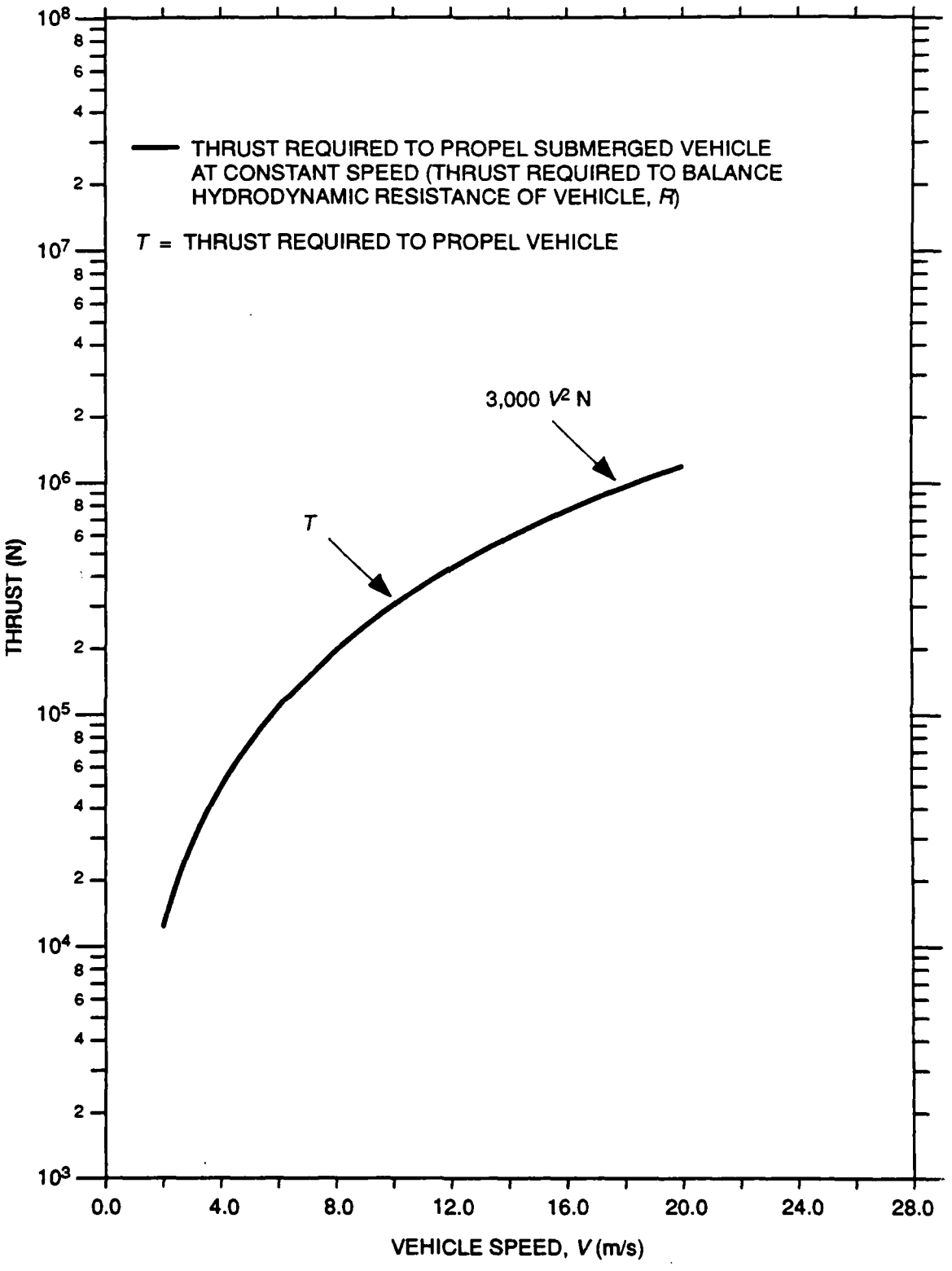

Fig. 9. Thrust required to propel submerged vehicle at constant speed *V*.

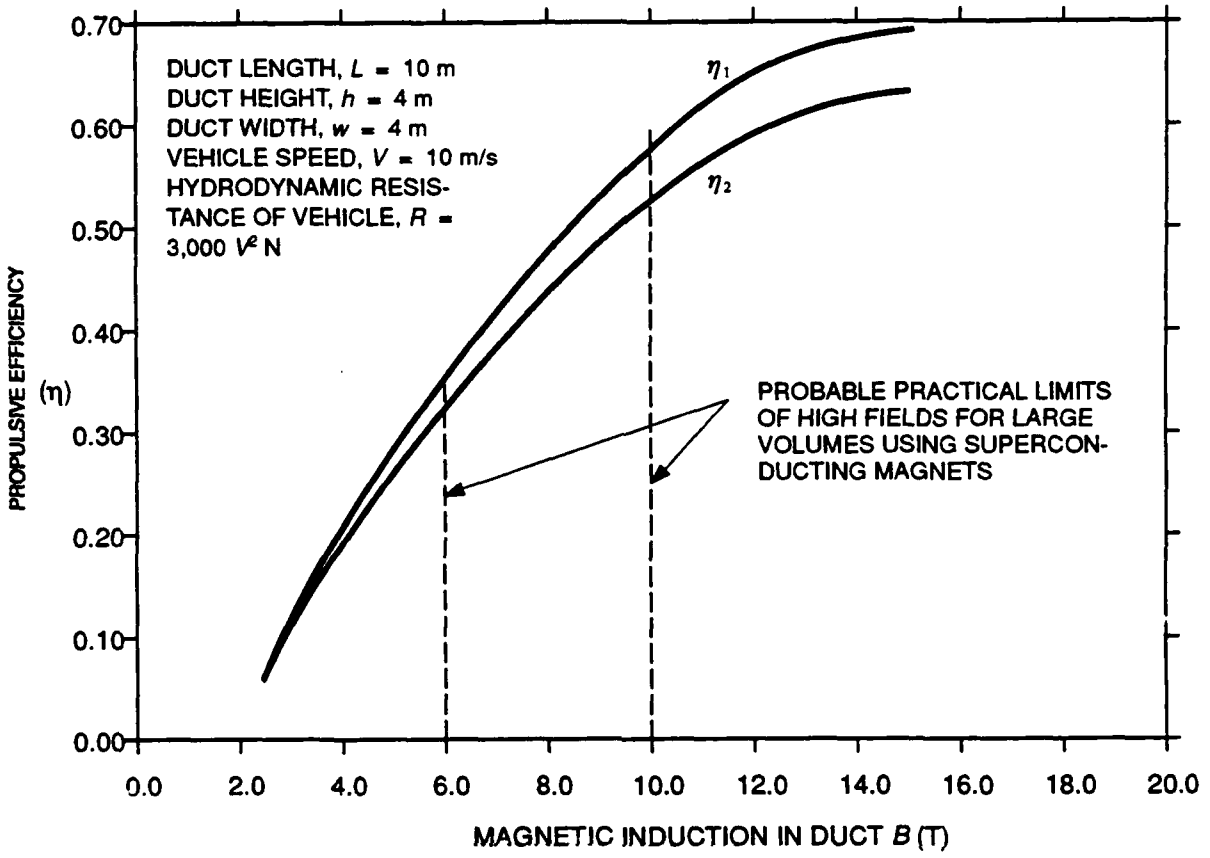

Fig. 10. Propulsive efficiency of square MHD duct versus magnetic induction in tesla.

32 m. The MHD duct length L was maintained at 10 m. On each figure two groups of numerical curves for submerged vehicle speeds of 2.5, 5, and 10 m/second are presented for magnetic inductions of 6 and 10 tesla. The vessel hydrodynamic resistance was 3000 V^2 newtons. The corresponding propulsive efficiency curves η_1 on each figure for identical submerged vehicle speed have higher η_1 values at 10 tesla than at 6 tesla on each figure, as would be expected. On each figure the propulsive efficiency values η_1 of each curve increases with duct height h when h increases from 4 to roughly 10 m and then decreases slightly to 32 m. The main point that each figure shows is that the corresponding propulsive efficiency curve values η_1 increase with duct width w.

The propulsive efficiency η_1 can be derived from Eq. 39 and 44 to be

$$\eta_1 = \frac{TV}{I\phi} = \left\{ BV - \frac{(1/8)\, f\varrho V_D^2 V 2L \ \left[1 + (h/w)\right]}{I} \right\} \left(\frac{I}{Lh\sigma} + V_D B \right)^{-1}, \qquad (47)$$

where the current I in the channel is determined from

$$I = \frac{T}{Bw} + \frac{L\varrho}{4B}\left(1 + \frac{h}{w}\right) fV_D^2 \quad . \tag{48}$$

In Eq. 47, the frictional term containing the friction factor f is much smaller than BV, and in Eq. 48 the friction term containing f is much smaller than T/Bw, since L is only 10 m. Increasing L to large values will significantly increase the frictional resistance in the MHD duct. From Eq. 48 it can be seen that increasing w decreases I, the total current in the duct, which increases η_1 in Eq. 47, as the numerical results show.

The MHD propulsive efficiencies reported here which approach those of a propeller correspond to duct volumes greater than 160 m^3, with small surface area-to-volume ratios. These large-volume magnetic inductions of 6 to 10 tesla may be unattainable in practice.

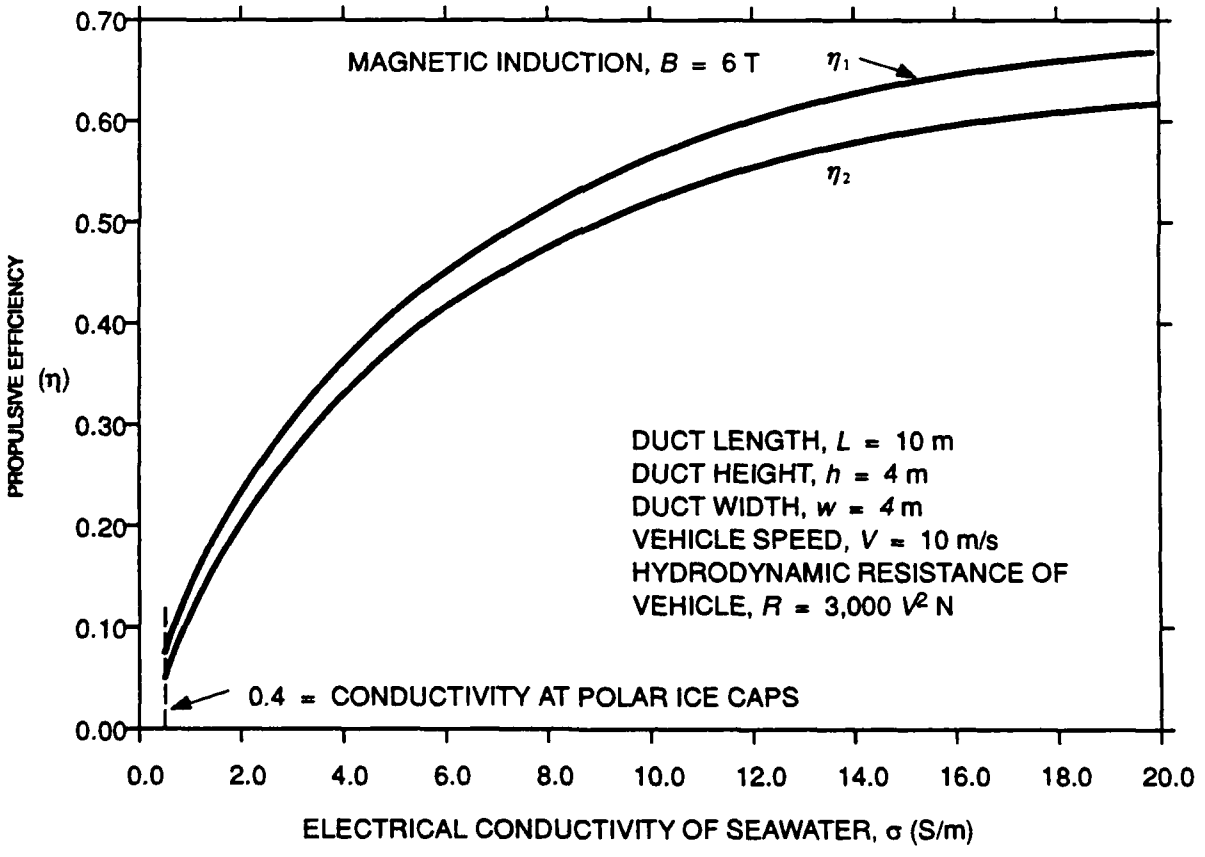

Fig. 11. Propulsive efficiency versus electrical conductivity of seawater. (Electrical conductivity of normal seawater is approximately 4 S/m.)

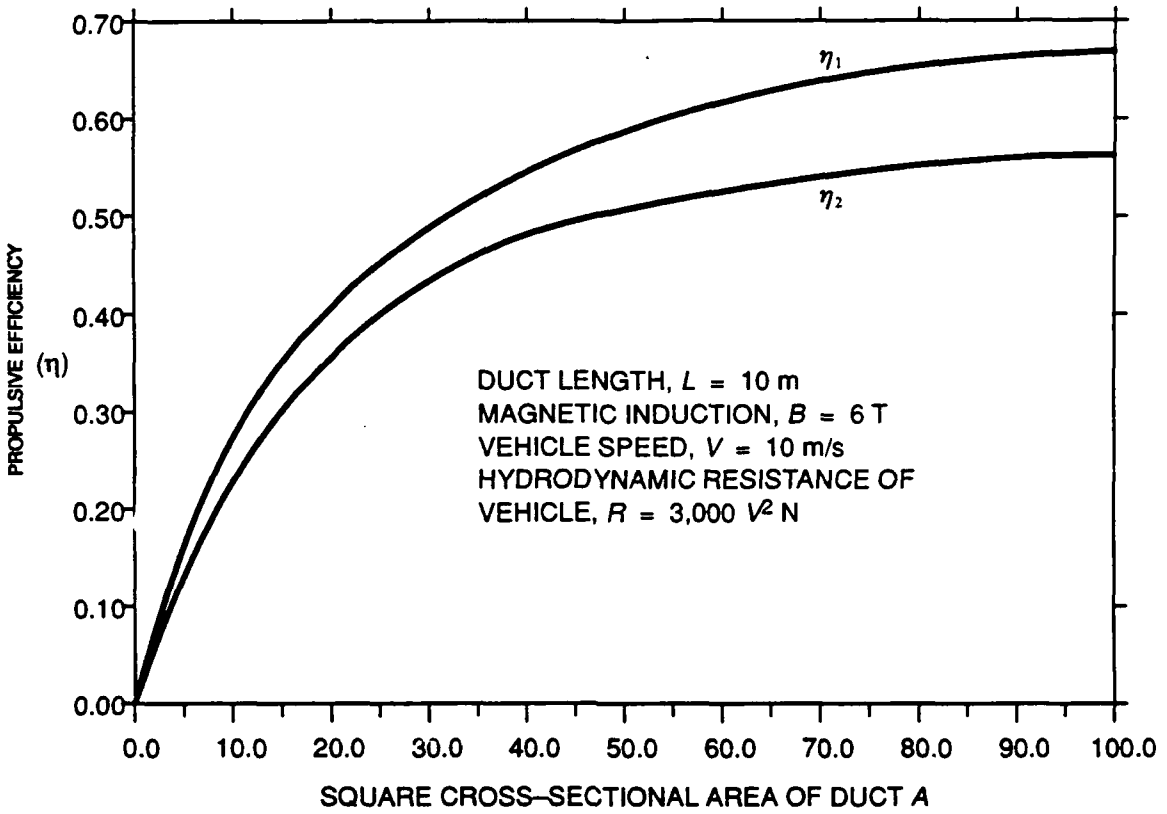

Fig. 12. Propulsive efficiency of square MHD duct versus duct cross-sectional area.

Tables 2 to 4 present the propulsive efficiencies η_1 for different length L square ducts having height h of 4 m and width w of 4 m versus vehicle speed V in meters per second. (Note: 1 m/second = 1.944 knots.) The magnetic induction B across the duct is 2 tesla in Table 2, 6 tesla in Table 3, and 10 tesla in Table 4. The hydrodynamic resistance of the submerged vehicle is 3000 V^2 newtons and thus requires a power of 3000 V^3 watts to propel the vehicle at a constant speed V. The propulsive efficiency η_1 increases significantly with an increase in magnetic induction B. Bear in mind that a magnetic induction of 6 to 10 tesla across the duct is a practical upper limit, imposed mainly through structural considerations using available superconducting magnet technology. The efficiency η_1 decreases significantly with decreasing vehicle speed V. For the 2–tesla magnetic induction B the efficiency η_1 tends to increase slightly as duct length increases to 40 m. For the 6–tesla magnetic induction the efficiency generally tends to increase slowly with duct length L to 40 m. With the 10 tesla magnetic induction B the efficiency η_1 generally tends to increase slowly with duct length L to 40 m. In these numerical calculations the conductivity of seawater σ was assumed to be 4 siemens/m.

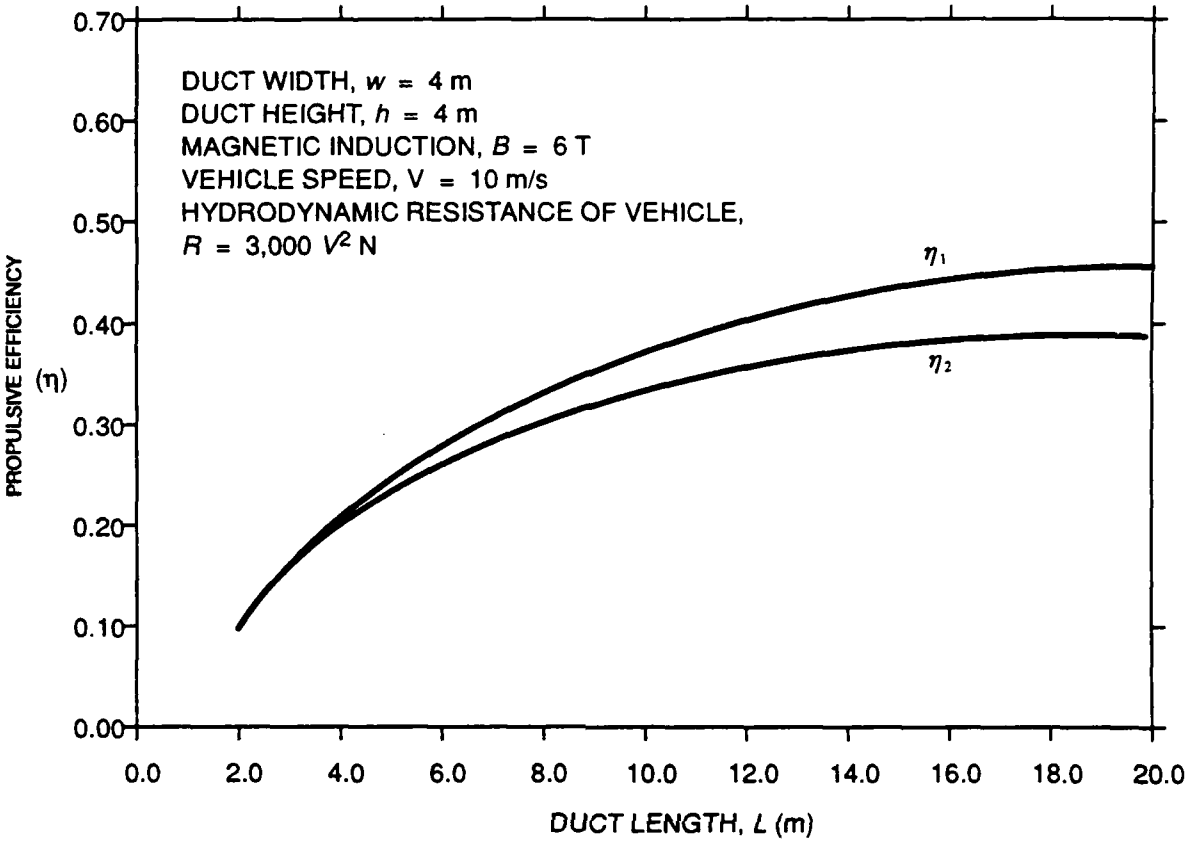

Fig. 13. Propulsive efficiency of square duct versus duct length.

Tables 5 and 6 present the propulsive efficiencies η_1 for the rectangular duct of width w of 4 m and height h of 4 m versus duct length L in meters and vehicle speed V in meters per second for magnetic inductions B of 6 and 10 tesla, respectively. The tables show that extremely long duct lengths L of over 50 m generally degrade the propulsive efficiency η_1 with the efficiency decreasing with increasing length. This would be expected since the propulsive efficiencies decrease because of the increased skin friction in the duct with increased surface area.

Table 7 presents the propulsive efficiency η_1 for the preceding MHD duct with a length L of 10 m versus vehicle speed V in meters per second and conductivity of seawater σ in siemens/meter. The magnetic induction across the duct is 6 tesla. The hydrodynamic resistance of the submerged vehicle in the seawater is 3000 V^2. The propulsive efficiency η_1 increased significantly with increases in fluid electrical conductivity σ and decreases in vehicle speed V. The conductivity of seawater can be increased by seeding. However, it does not appear that this is practical for MHD propulsion.

Table 8 presents the propulsive efficiency η_1 for the duct versus magnetic induction B across the duct and conductivity σ of the fluid flowing through the duct. The hydrodynamic resistance of the submerged vehicle in seawater is 3000 V^2 newtons. The propulsive efficiency η_1 increases significantly with increasing fluid conductivity σ and increasing magnetic induction B. However, the conductivity of seawater is generally about 4 siemens per meter and the practical limit to B is about 10 tesla with today's present superconducting magnet technology.

Tables 9 through 13 present the propulsive efficiency η_1 for the square MHD propulsive duct versus vehicle speed V in meters per second and magnetic induction B in tesla. The hydrodynamic resistance R of the vehicle is 1000 V^2 newtons in Table 9, 2000 V^2 newtons in Table 10, 3000 V^2 newtons in Table 11, 4000 V^2 newtons in Table 12, and 5000 V^2 in Table 13. For each table the propulsive efficiency η_1 increases with magnetic induction B and decreases with vehicle speed V in meters per second. These table also show that the propulsive efficiency η_1 for the MHD system generally increases as the hydrodynamic resistance of the submerged vehicle decreases.

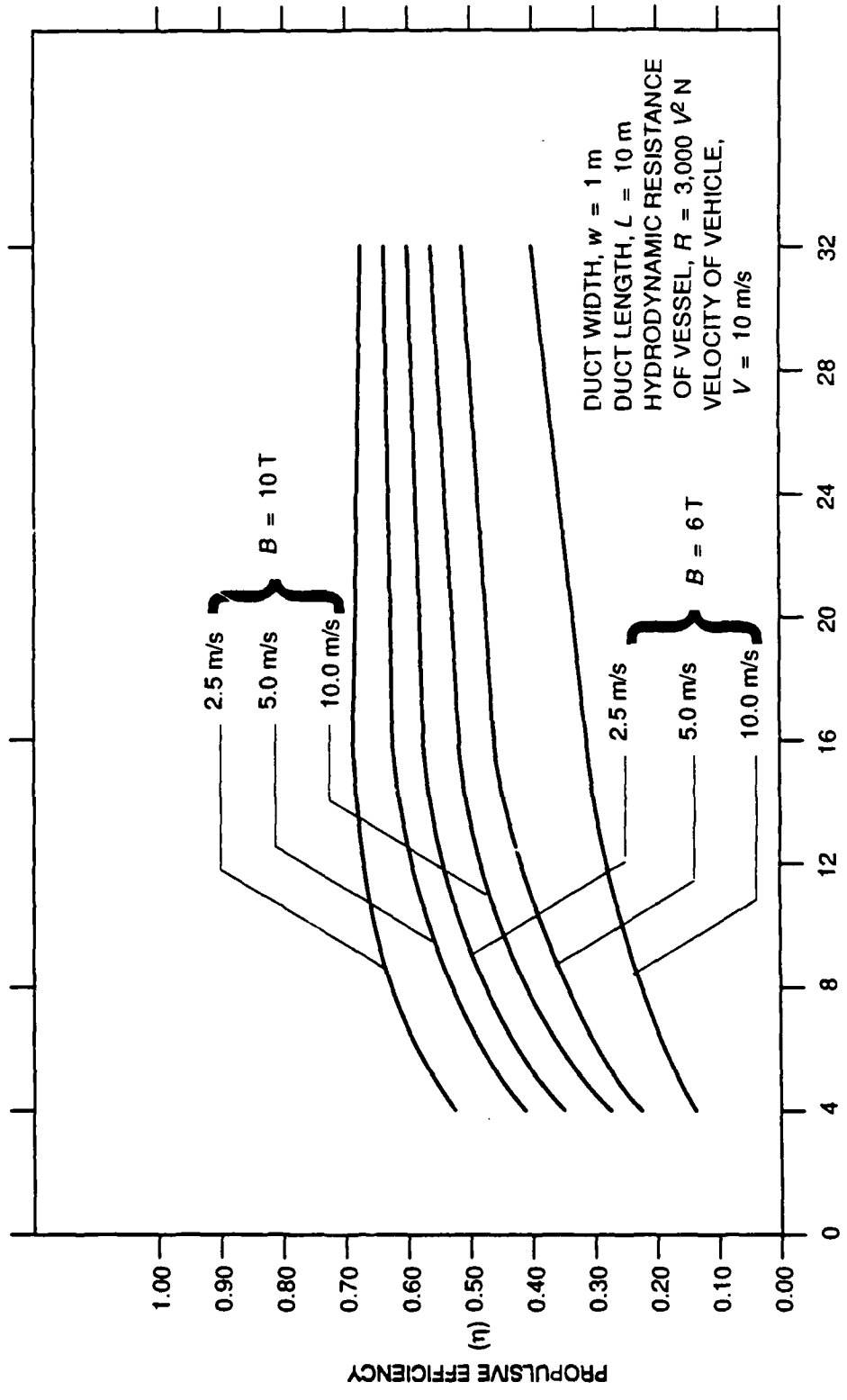

Fig. 14. Propulsive efficiency η_1 versus duct height (duct width w = 1 m).

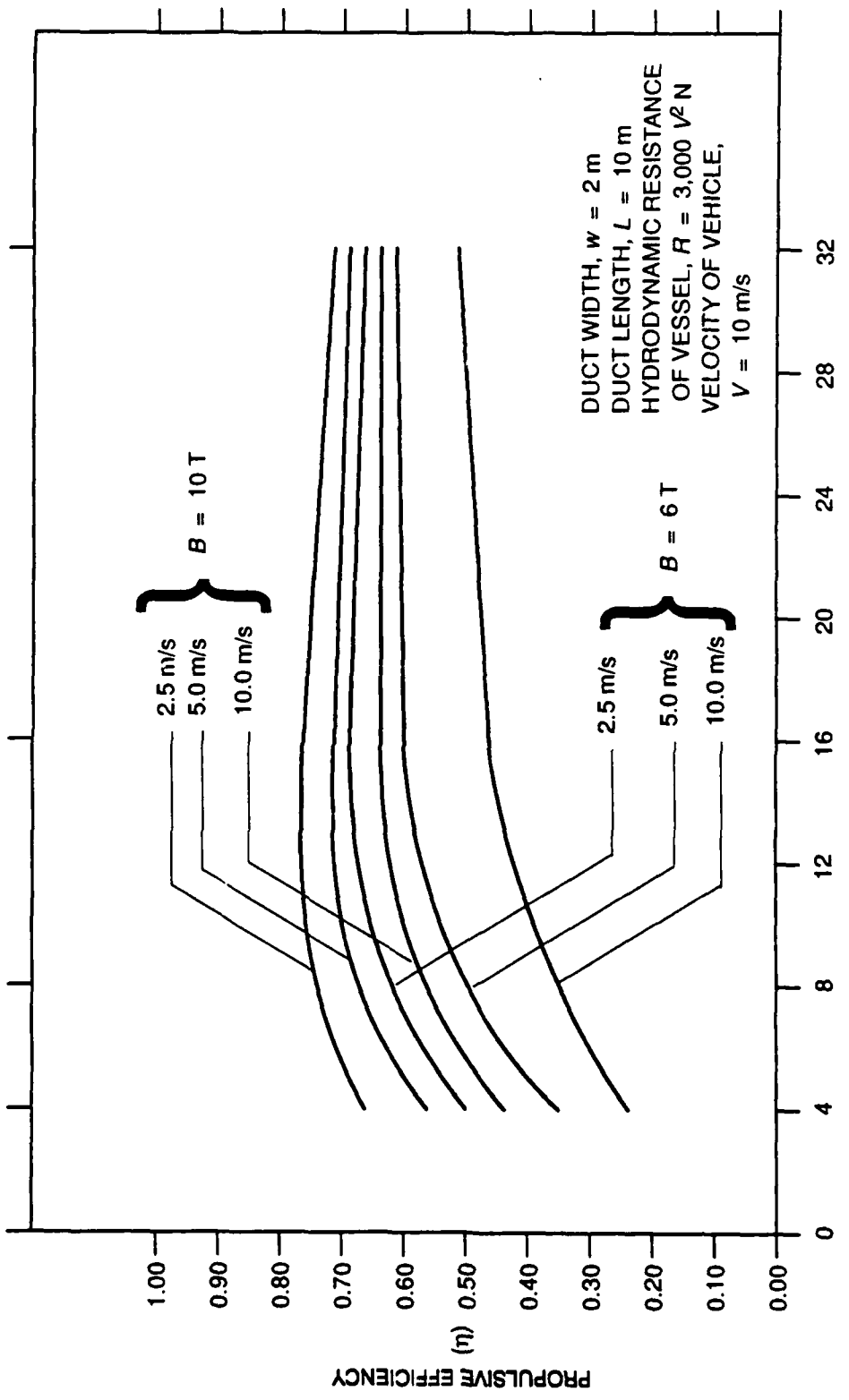

Fig. 15. Propulsive efficiency η_1 versus duct height (duct width w = 2 m).

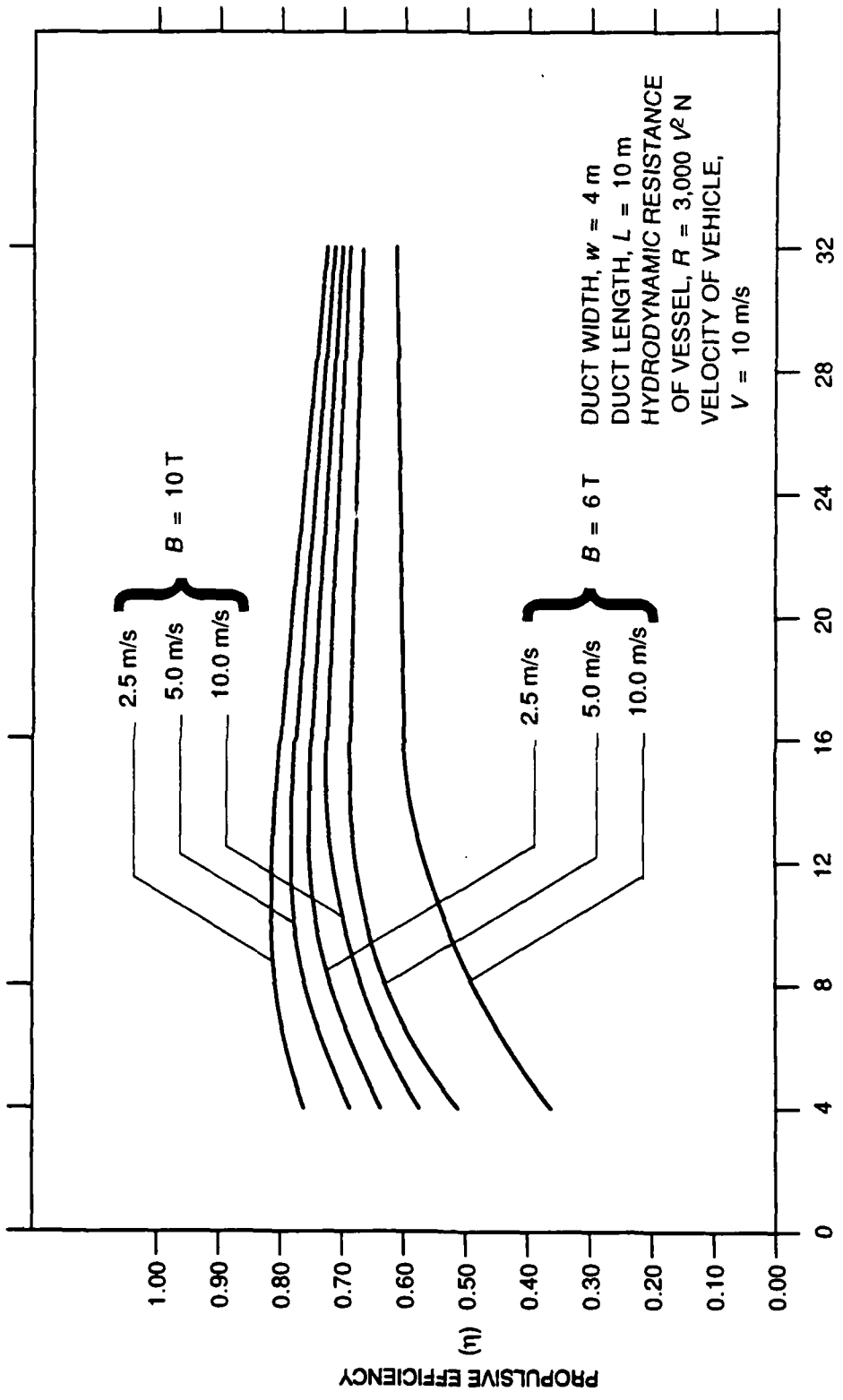

Fig. 16. Propulsive efficiency η_1 versus duct height (duct width $w = 4$ m).

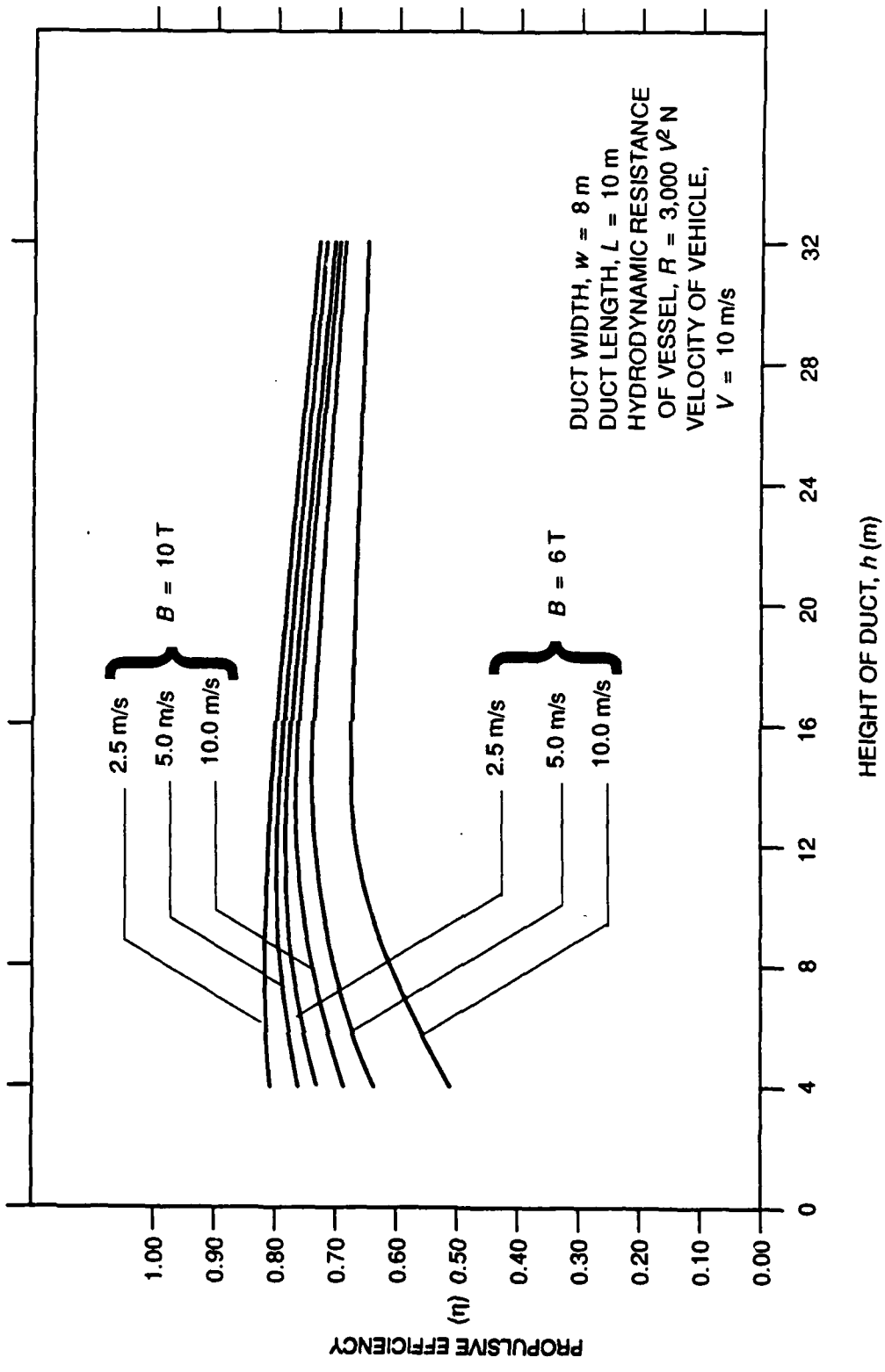

Fig. 17. Propulsive efficiency η_1 versus duct height (duct width $w = 8$ m).

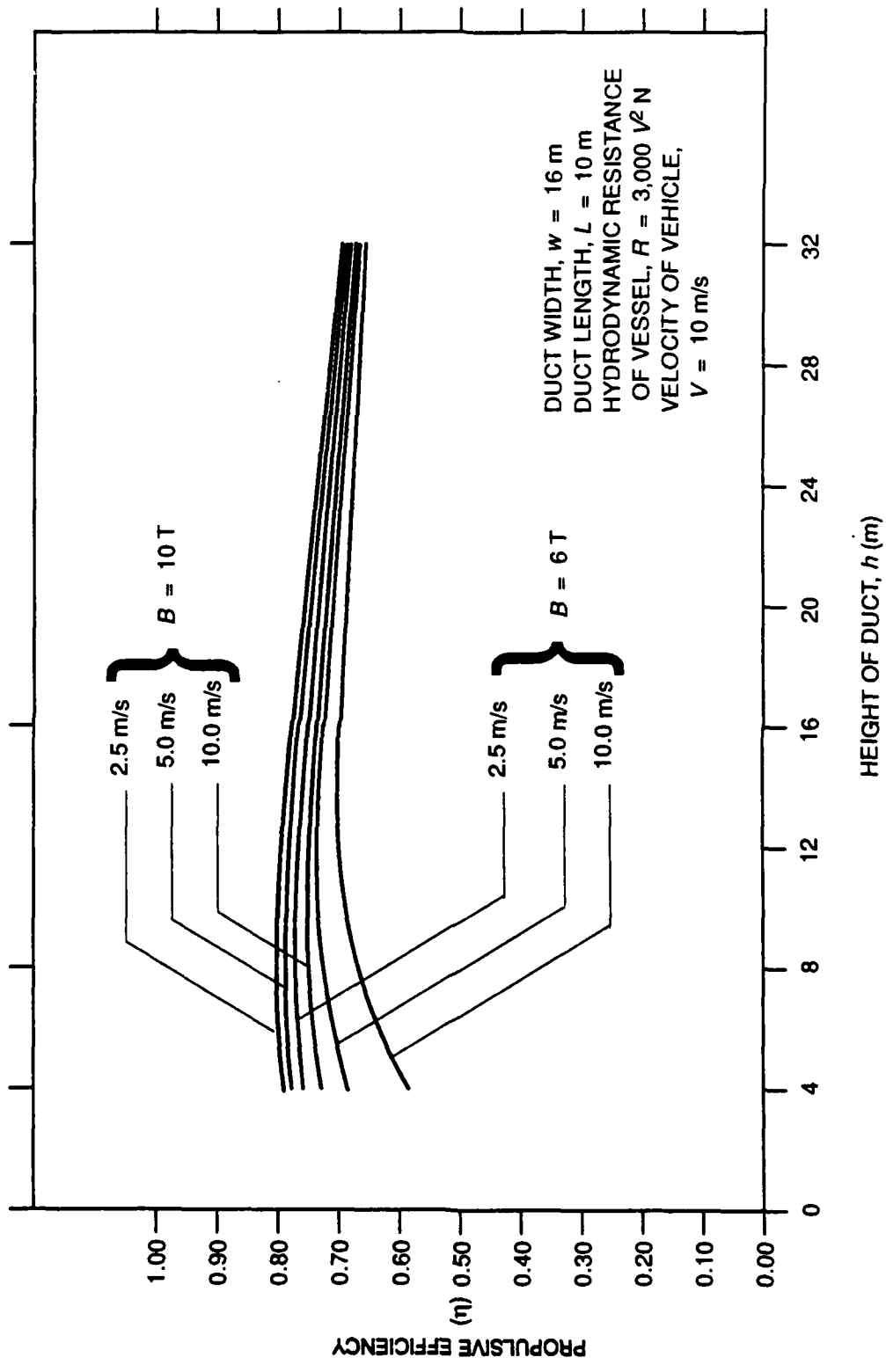

Fig. 18. Propulsive efficiency η_1 versus duct height (duct width w = 16 m).

Table 2. Propulsive efficiency $\eta_1 \times 10^2$ versus submerged vehicle speed and length of square duct at 2 tesla. (Duct height $h = 4$ meters, duct width $w = 4$ meters, magnetic induction in duct $B = 2$ tesla, hydrodynamic resistance $R = 3000\ V^2$ newtons, skin friction coefficient in duct $C_{fd} = 0.00262$. Velocity of submerged vehicle V in meters per second; length of duct L in meters.)

$V =$	2	4	6	8	10	12	14	16	18	20	22	24	26	28	30	32	34	36	38	40
$L = 2$	7.6	3.9	2.7	2.0	1.6	1.4	1.2	1.0	0.9	0.8	0.7	0.7	0.6	0.6	0.5	0.5	0.5	0.5	0.4	0.4
$L = 4$	13.5	7.3	5.0	3.8	3.1	2.6	2.2	2.0	1.7	1.6	1.4	1.3	1.2	1.1	1.1	1.0	0.9	0.9	0.8	0.8
$L = 6$	18.3	10.2	7.1	5.4	4.4	3.7	3.2	2.8	2.5	2.3	2.1	1.9	1.7	1.6	1.5	1.4	1.3	1.3	1.2	1.1
$L = 8$	22.2	12.8	9.0	6.9	5.6	4.7	4.1	3.6	3.2	2.9	2.6	2.4	2.2	2.1	2.0	1.8	1.7	1.6	1.5	1.5
$L = 10$	25.4	15.0	10.6	8.2	6.7	5.6	4.9	4.3	3.8	3.4	3.2	2.9	2.7	2.5	2.4	2.2	2.1	2.0	1.9	1.8
$L = 12$	28.1	16.9	12.1	9.4	7.7	6.5	5.6	5.0	4.4	4.0	3.7	3.4	3.1	2.9	2.7	2.6	2.4	2.3	2.2	2.1
$L = 14$	30.3	18.5	13.4	10.4	8.6	7.3	6.3	5.6	5.0	4.5	4.1	3.8	3.5	3.3	3.1	2.9	2.7	2.6	2.4	2.3
$L = 16$	32.1	20.0	14.5	11.4	9.4	8.0	6.9	6.1	5.5	5.0	4.5	4.2	3.9	3.6	3.4	3.2	3.0	2.8	2.7	2.6
$L = 18$	33.6	21.3	15.6	12.3	10.1	8.6	7.5	6.6	6.0	5.4	4.9	4.6	4.2	3.9	3.7	3.5	3.3	3.1	2.9	2.8
$L = 20$	34.9	22.4	16.5	13.0	10.8	9.2	8.0	7.1	6.4	5.8	5.3	4.9	4.5	4.2	4.0	3.7	3.5	3.3	3.2	3.0
$L = 22$	35.9	23.4	17.3	13.7	11.4	9.7	8.5	7.5	6.8	6.2	5.6	5.2	4.8	4.5	4.2	4.0	3.7	3.5	3.4	3.2
$L = 24$	36.8	24.2	18.1	14.4	12.0	10.2	8.9	7.9	7.1	6.5	5.9	5.5	5.1	4.7	4.4	4.2	4.0	3.7	3.6	3.4
$L = 26$	37.6	25.0	18.7	15.0	12.5	10.7	9.3	8.3	7.5	6.8	6.2	5.7	5.3	5.0	4.7	4.4	4.1	3.9	3.7	3.6
$L = 28$	38.2	25.7	19.3	15.5	12.9	11.1	9.7	8.6	7.8	7.1	6.5	6.0	5.6	5.2	4.9	4.6	4.3	4.1	3.9	3.7
$L = 30$	38.7	26.2	19.9	16.0	13.4	11.5	10.1	9.0	8.1	7.3	6.7	6.2	5.8	5.4	5.1	4.8	4.5	4.3	4.1	3.9
$L = 32$	39.1	26.8	20.3	16.4	13.7	11.8	10.4	9.2	8.3	7.6	7.0	6.4	6.0	5.6	5.2	4.9	4.7	4.4	4.2	4.0
$L = 34$	39.4	27.2	20.8	16.8	14.1	12.1	10.7	9.5	8.6	7.8	7.2	6.6	6.2	5.8	5.4	5.1	4.8	4.6	4.3	4.1
$L = 36$	39.7	27.6	21.1	17.1	14.4	12.4	10.9	9.7	8.8	8.0	7.4	6.8	6.3	5.9	5.6	5.2	4.9	4.7	4.5	4.2
$L = 38$	39.9	27.9	21.5	17.4	14.7	12.7	11.2	10.0	9.0	8.2	7.5	7.0	6.5	6.1	5.7	5.4	5.1	4.8	4.6	4.4
$L = 40$	40.0	28.2	21.8	17.7	15.0	12.9	11.4	10.2	9.2	8.4	7.7	7.1	6.6	6.2	5.8	5.5	5.2	4.9	4.7	4.5

Table 3. Propulsive efficiency $\eta_1 \times 10^2$ versus submerged vehicle speed and length of square duct at 6 tesla. . (Duct height $h = 4$ meters, duct width $w = 4$ meters, magnetic induction in duct $B = 6$ tesla, hydrodynamic resistance $R = 3000\ V^2$ newtons, skin friction coefficient in duct $C_{fd} = 0.00262$. Velocity of submerged vehicle V in meters per second; length of duct L in meters.)

$V=$	2	4	6	8	10	12	14	16	18	20	22	24	26	28	30	32	34	36	38	40
$L=2$	40.8	26.3	19.4	15.4	12.8	10.9	9.5	8.4	7.6	6.9	6.3	5.8	5.4	5.0	4.7	4.4	4.2	3.9	3.7	3.6
$L=4$	55.1	39.8	31.2	25.6	21.7	18.9	16.7	15.0	13.5	12.4	11.4	10.6	9.8	9.2	8.8	8.2	7.7	7.3	7.0	6.7
$L=6$	61.8	47.7	38.8	32.7	28.3	24.9	22.3	20.1	18.3	16.9	15.6	14.5	13.6	12.7	12.0	11.4	10.8	10.2	9.8	9.3
$L=8$	65.4	52.7	44.1	37.9	33.2	29.6	26.6	24.2	22.2	20.5	19.1	17.8	16.7	15.7	14.9	14.1	13.4	12.8	12.2	11.7
$L=10$	67.5	55.9	47.8	41.7	36.9	33.2	30.1	27.6	25.4	23.6	22.0	20.6	19.4	18.3	17.3	16.5	15.7	15.0	14.3	13.7
$L=12$	68.6	58.1	50.4	44.5	39.8	36.1	32.9	30.3	28.1	26.1	24.5	23.0	21.7	20.5	19.5	18.5	17.6	16.9	16.1	15.5
$L=14$	69.2	59.6	52.4	46.7	42.1	38.4	35..2	32.6	30.3	28.3	26.5	25.0	23.6	22.4	21.3	20.3	19.4	18.5	17.8	17.1
$L=16$	69.4	60.6	53.8	48.3	43.9	40.2	37.1	34.4	32.1	30.1	28.3	26.7	25.3	24.0	22.9	21.8	20.9	20.0	19.2	18.4
$L=18$	69.4	61.3	54.8	49.6	45.3	41.7	38.6	35.9	33.6	31.6	29.8	28.2	26.7	25.4	24.2	23.2	22.2	21.3	20.4	19.7
$L=20$	69.2	61.6	55.5	50.6	46.4	42.8	39.8	37.2	34.9	32.8	31.0	29.4	27.9	26.6	25.4	24.3	23.3	22.4	21.5	20.7
$L=22$	68.9	61.8	56.0	51.3	47.2	43.8	40.8	38.2	35.9	33.9	32.1	30.5	29.0	27.7	26.5	25.3	24.3	23.4	22.5	21.7
$L=24$	68.5	61.8	56.4	51.8	47.9	44.6	41.6	39.1	36.8	34.8	33.0	31.4	29.9	28.6	27.4	26.2	25.2	24.2	23.3	22.5
$L=26$	68.0	61.7	56.5	52.2	48.4	45.1	42.3	39.8	37.6	35.6	33.8	32.2	30.7	29.4	28.1	27.0	26.0	25.0	24.1	23.3
$L=28$	67.5	61.6	56.6	52.4	48.8	45.6	42.8	40.4	38.2	36.2	34.4	32.8	31.4	30.0	28.8	27.7	26.6	25.7	24.8	23.9
$L=30$	66.9	61.3	56.6	52.5	49.0	46.0	43.3	40.8	38.7	36.8	35.0	33.4	32.0	30.6	29.4	28.3	27.2	26.2	25.3	24.5
$L=32$	66.3	61.0	56.5	52.6	49.2	46.2	43.6	41.2	39.1	37.2	35.5	33.9	32.4	31.1	29.9	28.8	27.7	26.8	25.8	25.0
$L=34$	65.7	60.7	56.3	52.6	49.3	46.4	43.8	41.5	39.4	37.6	35.8	34.3	32.9	31.5	30.3	29.2	28.2	27.2	26.3	25.4
$L=36$	65.1	60.3	56.1	52.5	49.3	46.5	44.0	41.7	39.7	37.8	36.2	34.6	33.2	31.9	30.7	29.6	28.6	27.6	26.7	25.8
$L=38$	64.5	59.9	55.9	52.4	49.3	46.6	44.1	41.9	39.9	38.1	36.4	34.9	33.5	32.3	31.0	29.9	28.9	27.9	27.0	26.2
$L=40$	63.8	59.4	55.6	52.2	49.2	46.6	44.2	42.0	40.0	38.3	36.6	35.1	33.8	32.5	31.3	30.2	29.2	28.2	27.3	26.5

Table 4. Propulsive efficiency $\eta_1 \times 10^2$ versus submerged vehicle speed and length of square duct at 10 tesla. (Duct height $h = 4$ meters, duct width $w = 4$ meters, magnetic induction in duct $B = 10$ tesla, hydrodynamic resistance $R = 3000\ V^2$ newtons, skin friction coefficient in duct $C_{fd} = 0.00262$. Velocity of submerged vehicle V in meters per second; length of duct L in meters.)

V=	2	4	6	8	10	12	14	16	18	20	22	24	26	28	30	32	34	36	38	40
$L = 2$	63.0	48.3	39.1	32.9	28.4	24.9	22.2	20.1	18.3	16.8	15.5	14.5	13.5	12.7	11.9	11.3	10.7	10.2	9.7	9.3
$L = 4$	72.9	61.7	53.4	47.1	42.1	38.1	34.8	32.0	29.6	27.6	25.8	24.2	22.8	21.6	20.5	19.5	18.6	17.8	17.0	16.3
$L = 6$	76.2	67.4	60.4	54.7	50.0	46.0	42.6	39.7	37.2	34.9	32.9	31.2	29.6	28.1	26.8	25.7	24.6	23.6	22.6	21.8
$L = 8$	77.5	70.2	64.2	59.1	54.8	51.1	47.8	44.9	42.4	40.1	38.1	36.2	34.6	33.0	31.6	30.4	29.2	28.1	27.1	26.1
$L = 10$	77.8	71.6	66.4	61.9	57.9	54.4	51.4	48.6	46.1	43.9	41.9	40.0	38.3	36.8	35.3	34.0	32.8	31.6	30.6	29.6
$L = 12$	77.6	72.3	67.7	63.6	60.0	56.7	53.9	51.2	48.9	46.7	44.7	42.9	41.2	39.7	38.2	36.9	35.7	34.5	33.4	32.4
$L = 14$	77.2	72.5	68.3	64.6	61.3	58.3	55.6	53.1	50.9	48.8	46.9	45.1	43.5	41.9	40.5	39.2	37.9	36.8	35.7	34.6
$L = 16$	76.6	72.4	68.6	65.3	62.2	59.4	56.9	54.5	52.4	50.4	48.5	46.8	45.2	43.7	42.3	41.0	39.8	38.6	37.5	36.5
$L = 18$	75.9	72.1	68.7	65.6	62.7	60.1	57.7	55.5	53.5	51.6	49.8	48.1	46.6	45.1	43.8	42.5	41.3	40.1	39.0	38.0
$L = 20$	75.1	71.7	68.5	65.7	63.0	60.6	58.3	56.2	54.3	52.4	50.7	49.1	47.6	46.2	44.9	43.6	42.5	41.3	40.3	39.3
$L = 22$	74.3	71.2	68.3	65.6	63.1	60.8	58.7	56.7	54.8	53.1	51.4	49.9	48.5	47.1	45.8	44.6	43.4	42.3	41.3	40.3
$L = 24$	73.5	70.6	67.9	65.4	63.1	60.9	58.9	57.0	55.2	53.5	52.0	50.5	49.1	47.8	46.5	45.3	44.2	43.1	42.1	41.1
$L = 26$	72.7	70.0	67.4	65.1	62.9	60.8	58.9	57.1	55.4	53.8	52.3	50.9	49.5	48.3	47.0	45.9	44.8	43.7	42.7	41.8
$L = 28$	71.9	69.3	67.0	64.7	62.7	60.7	58.9	57.2	55.5	54.0	52.6	51.2	49.9	48.6	47.5	46.3	45.3	44.2	43.3	42.3
$L = 30$	71.1	68.7	66.4	64.3	62.4	60.5	58.8	57.1	55.6	54.1	52.7	51.4	50.1	48.9	47.8	46.7	45.6	44.6	43.7	42.7
$L = 32$	70.2	68.0	65.9	63.9	62.0	58.6	57.0	55.5	55.5	54.1	52.7	51.5	50.2	49.1	48.0	46.9	45.9	44.9	44.0	43.1
$L = 34$	69.4	67.3	65.3	63.4	61.6	59.9	58.3	56.8	55.4	54.0	52.7	51.5	50.3	49.2	48.1	47.1	46.1	45.1	44.2	43.3
$L = 36$	68.6	66.6	64.7	62.9	61.2	59.6	58.0	56.6	55.2	53.9	52.6	51.4	50.3	49.2	48.2	47.1	46.2	45.3	44.4	43.5
$L = 38$	67.8	65.9	64.1	62.4	60.7	59.2	57.7	56.3	55.0	53.7	52.5	51.3	50.2	49.2	48.2	47.2	46.2	45.3	44.5	43.6
$L = 40$	67.0	65.2	63.5	61.8	60.3	58.8	57.4	56.0	54.7	53.5	52.3	51.2	50.1	49.1	48.1	47.2	46.3	45.4	44.5	43.7

Table 5. Propulsive efficiency $\eta_1 \times 10^2$ versus submerged vehicle speed and length of square duct at 6 tesla. (Duct height $h = 4$ meters, duct width $w = 4$ meters, magnetic induction in duct $B = 6$ tesla, hydrodynamic resistance $R = 3000\ V^2$ newtons, skin friction coefficient in duct $C_{fd} = 0.00262$. Velocity of submerged vehicle V in meters per second; length of duct L in meters.)

$V =$	5	10	15	20	25	30	35	40	45	50
$L = 25$	59.0	48.2	40.7	35.2	31.0	27.8	25.1	22.9	21.1	19.5
$L = 50$	55.4	48.4	42.9	38.6	35.0	32.1	29.6	27.4	25.6	24.0
$L = 75$	50.0	44.8	40.6	37.1	34.2	31.7	29.5	27.6	26.0	24.5
$L = 100$	45.1	41.0	37.6	34.7	32.2	30.1	28.2	26.5	25.1	23.8
$L = 125$	40.9	37.5	34.7	32.2	30.1	28.2	26.6	25.1	23.8	22.6
$L = 150$	37.3	34.5	32.0	29.9	28.0	26.4	24.9	23.6	22.4	21.4
$L = 175$	34.4	31.9	29.7	27.8	26.2	24.7	23.4	22.2	21.1	20.2
$L = 200$	31.8	29.6	27.7	26.0	24.5	23.1	22.0	20.9	19.9	19.0
$L = 225$	29.6	27.6	25/9	24.3	23.0	21.8	20.7	19.7	18.8	18.0
$L = 250$	27.6	25.8	24.3	22.9	21.6	20.5	19.5	18.6	17.8	17.0
$L = 275$	25.9	24.3	22.8	21.6	20.4	19.4	18.4	17.6	16.8	16.1
$L = 300$	24.4	22.9	21.6	20.4	19.3	18.4	17.5	16.7	16.0	15.3
$L = 325$	23.1	21.7	20.4	19.3	18.3	17.4	16.6	15.9	15.2	14.6
$L = 350$	21.9	20.6	19.4	18.4	17.4	16.6	15.8	15.1	14.5	13.9
$L = 375$	20.8	19.6	18.5	17.5	16.6	15.8	15.1	14.5	13.9	13.3
$L = 400$	19.8	18.7	17.6	16.7	15.9	15.1	14.5	13.8	13.3	12.7
$L = 425$	18.9	17.8	16.9	16.0	15.2	14.5	13.9	13.3	12.7	12.2
$L = 450$	18.1	17.1	16.1	15.3	14.6	13.9	13.3	12.7	12.2	11.7
$L = 475$	17.3	16.4	15.5	14.7	14.0	13.4	12.8	12.2	11.7	11.3
$L = 500$	16.6	15.7	14.9	14.1	13.5	12.9	12.3	11.8	11.3	10.9

Table 6. Propulsive efficiency $\eta_1 \times 10^2$ versus submerged vehicle speed and length of square duct at 10 tesla. (Duct height $h = 4$ meters, duct width $w = 4$ meters, magnetic induction in duct $B = 10$ tesla, hydrodynamic resistance $R = 3000\ V^2$ newtons, skin friction coefficient in duct $C_{fd} = 0.00262$. Velocity of submerged vehicle V in meters per second, length of duct L in meters.)

$V =$	5	10	15	20	25	30	35	40	45	50
$L = 25$	69.0	63.0	58.0	53.7	50.0	46.8	44.0	41.5	39.2	37.2
$L = 50$	61.1	57.8	54.8	52.1	49.6	47.4	45.4	43.5	41.8	40.2
$L = 75$	54.0	51.7	49.5	47.6	45.8	44.1	42.5	41.1	39.7	38.4
$L = 100$	48.1	46.4	44.7	43.2	41.7	40.4	39.1	38.0	36.8	35.8
$L = 125$	43.4	41.9	40.6	39.3	38.1	37.0	36.0	35.0	34.0	33.1
$L = 150$	39.4	38.2	37.1	36.0	35.0	34.1	33.2	32.3	31.5	30.7
$L = 175$	36.2	35.1	34.1	33.2	32.3	31.5	30.7	29.9	29.2	28.5
$L = 200$	33.4	32.5	31.6	30.8	30.0	29.2	28.5	27.9	27.2	26.6
$L = 225$	31.0	30.2	29.4	28.7	28.0	27.3	26.7	26.0	25.5	24.9
$L = 250$	28.9	28.2	27.5	26.8	26.2	25.6	25.0	24.4	23.9	23.4
$L = 275$	27.1	26.4	25.8	25.2	24.6	24.0	23.5	23.0	22.5	22.1
$L = 300$	25.5	24.9	24.3	23.7	23.2	22.7	22.2	21.7	21.3	20.8
$L = 325$	24.1	23.5	23.0	22.4	21.9	21.5	21.0	20.6	20.2	19.8
$L = 350$	22.8	22.3	21.8	21.3	20.8	20.4	19.9	19.5	19.1	18.8
$L = 375$	21.6	21.2	20.7	20.2	19.8	19.4	19.0	18.6	18.2	17.9
$L = 400$	20.6	20.1	19.7	19.3	18.9	18.5	18.1	17.7	17.4	17.1
$L = 425$	19.7	19.2	18.8	18.4	18.0	17.7	17.3	17.0	16.6	16.3
$L = 450$	18.8	18.4	18.0	17.6	17.3	16.9	16.6	16.3	15.9	15.6
$L = 475$	18.0	17.6	17.3	16.9	16.6	16.2	15.9	15.6	15.3	15.0
$L = 500$	17.3	16.9	16.6	16.2	15.9	15.6	15.3	15.0	14.7	14.4

Table 7. Propulsive efficiency $\eta_1 \times 10^2$ versus electrical conductivity and submerged vehicle speed. (Duct height h = 4 meters, duct width w = 4 meters, duct length L = 10 meters, magnetic induction in duct B = 6 tesla, hydrodynamic resistance $R = 3000\ V^2$ newtons. Conductivity of seawater σ in siemens per meter; speed of submerged vehicle V in meters per second).

σ =	2	4	6	8	10	12	14	16	18	20	22	24	26	28	30	32	34	36	38	40
V = 2	55	67	72	75	77	78	79	79	80	80	81	81	81	82	82	82	82	82	82	82
V = 4	41	55	63	67	70	72	74	75	76	77	77	78	78	79	79	79	80	80	80	80
V = 6	33	47	55	61	64	67	69	71	72	73	74	75	75	76	77	77	77	78	78	78
V = 8	27	41	50	55	60	63	65	67	69	70	71	72	73	74	74	75	75	76	76	77
V = 10	23	36	45	51	55	59	61	64	65	67	68	69	70	71	72	73	73	74	74	75
V = 12	20	33	41	47	52	55	58	61	63	64	66	67	68	69	70	71	71	72	73	73
V = 14	18	30	38	44	49	52	55	58	60	62	63	65	66	67	68	69	70	70	71	71
V = 16	16	27	35	41	46	50	53	55	58	60	61	63	64	65	66	67	68	69	69	70
V = 18	14	25	33	39	43	47	50	53	55	57	59	61	62	63	64	65	66	67	68	68
V = 20	13	23	31	36	41	45	48	51	53	55	57	59	60	61	63	64	65	65	66	67
V = 22	12	22	29	34	39	43	46	49	51	54	55	57	59	60	61	62	63	64	65	66
V = 24	11	20	27	33	37	41	44	47	50	52	54	55	57	58	60	61	62	63	64	64
V = 26	10	19	26	31	36	39	43	46	48	50	52	54	55	57	58	59	60	61	62	63
V = 28	10	18	24	30	34	38	41	44	46	49	51	52	54	55	57	58	59	60	61	62
V = 30	9	17	23	28	33	36	40	43	45	47	49	51	53	54	55	57	58	59	60	61
V = 32	9	16	22	27	31	35	38	41	44	46	48	50	51	53	54	55	57	58	59	60
V = 34	8	15	21	26	30	34	37	40	42	45	47	48	50	52	53	54	55	57	58	58
V = 36	8	14	20	25	29	33	36	39	41	43	45	47	49	50	52	53	54	55	56	57
V = 38	7	14	19	24	28	32	35	38	40	42	44	46	48	49	51	52	53	54	55	56
V = 40	7	13	19	23	27	31	34	36	39	41	43	45	47	48	50	51	52	53	54	55

Table 8. Propulsive efficiency η_1 versus electrical conductivity and magnetic induction of square duct. (Duct height $h = 4$ meters, duct width $w = 4$ meters, duct length $L = 10$ meters, hydrodynamic resistance $R = 3000\ V^2$ newtons, velocity = 10 meters per second. Conductivity of seawater σ in siemens per meter; magnetic induction B in tesla.)

σ =	2	4	6	8	10	12	14	16	18	20	22	24	26	28	30	32	34	36	38	40
$B = 2$	3	6	9	12	14	17	19	21	23	25	27	28	30	31	33	34	35	36	38	40
$B = 4$	12	21	28	34	39	43	46	49	51	53	55	57	58	59	61	62	63	64	65	65
$B = 6$	23	36	45	51	55	59	61	64	65	67	68	69	70	71	72	73	73	74	74	75
$B = 8$	34	49	57	62	65	68	70	71	73	74	75	75	76	77	77	77	78	78	78	79
$B = 10$	43	57	64	68	71	73	75	76	77	77	78	78	79	79	80	80	80	80	81	81
$B = 12$	51	64	69	73	75	76	77	78	79	79	80	80	81	81	81	81	81	82	82	82
$B = 14$	57	68	73	75	77	78	79	80	80	81	81	81	82	82	82	82	82	82	82	83
$B = 16$	62	71	75	77	79	80	80	81	81	82	82	82	82	82	83	83	83	83	83	83
$B = 18$	65	74	77	79	80	81	81	82	82	82	82	83	83	83	83	83	83	83	83	83
$B = 20$	68	76	78	80	81	81	82	82	82	83	83	83	83	83	83	83	83	83	84	84
$B = 22$	71	77	79	81	81	82	82	83	83	83	83	83	83	83	83	84	84	84	84	84
$B = 24$	73	78	80	81	82	82	83	83	83	83	83	83	84	84	84	84	84	84	84	84
$B = 26$	74	79	81	82	82	83	83	83	83	83	84	84	84	84	84	84	84	84	84	84
$B = 28$	75	80	81	82	83	83	83	83	83	84	84	84	84	84	84	84	84	84	84	84
$B = 30$	77	80	82	83	83	83	83	84	84	84	84	84	84	84	84	84	84	84	84	84
$B = 32$	77	81	82	83	83	83	83	84	84	84	84	84	84	84	84	84	84	84	84	84
$B = 34$	78	81	82	83	83	83	84	84	84	84	84	84	84	84	84	84	84	84	84	84
$B = 36$	79	82	83	83	83	84	84	84	84	84	84	84	84	84	84	84	84	84	84	84
$B = 38$	79	82	83	83	83	84	84	84	84	84	84	84	84	84	84	84	84	84	84	84
$B = 40$	80	82	83	83	84	84	84	84	84	84	84	84	84	84	84	84	84	84	84	84

Table 9. Propulsive efficiency $\eta_1 \times 10^2$ versus hydrodynamic resistance of submerged vehicle (Duct height h = 4 meters, duct width w = 4 meters, duct length L = 10 meters, hydrodynamic resistance R = 1000 V^2 newtons. Velocity of submerged vehicle V in meters per second; magnetic induction B in tesla).

V=	2	4	6	8	10	12	14	16	18	20	22	24	26	28	30	32	34	36	38	40
B = 2	40.9	27.6	20.8	16.7	14.0	12.0	10.5	9.4	8.4	7.7	7.0	6.5	6.0	5.6	5.3	5.0	4.7	4.5	4.2	4.0
B = 4	64.2	54.0	46.6	40.9	36.5	33.0	30.1	27.6	25.5	23.8	22.2	20.8	19.6	18.6	17.6	16.7	15.9	15.2	14.6	14.0
B = 6	71.7	65.5	60.4	55.9	52/1	48.8	45.9	43.3	40.9	38.9	37.0	35.3	33.7	32.3	31.0	29.8	28.7	27.6	26.7	25.8
B = 8	74.7	70.8	67.3	64.2	61.3	58.6	56.2	54.0	51.9	50.0	48.2	46.6	45.0	43.6	42.2	40.9	39.7	38.6	37.5	36.5
B = 10	76.3	73.6	71.1	68.8	66.7	64.6	62.7	60.9	59.2	57.6	56.1	54.7	53.3	52.0	50.7	49.5	48.4	47.3	46.3	45.3
B = 12	77.1	75.2	73.4	71.7	70.0	68.5	67.0	65.5	64.2	62.8	61.6	60.4	59.2	58.1	57.0	55.9	54.9	54.0	53.0	52.1
B = 14	77.6	76.2	74.8	73.5	72.2	71.0	69.8	68.7	67.5	66.5	65.4	64.4	63.4	62.5	61.5	60.6	59.8	58.9	58.1	57.3
B = 16	78.0	76.9	75.8	74.7	73.7	72.7	71.8	70.8	69.9	69.0	68.2	67.3	65.5	65.7	64.9	64.2	63.4	62.7	62.0	61.3
B = 18	78.2	77.3	76.5	75.6	74.8	74.0	73.2	72.4	71.7	70.9	70.2	69.5	68.8	68.1	57.5	66.8	66.2	65.5	64.9	64.3
B = 20	78.4	77.6	76.9	76.3	75.6	74.9	74.3	73.6	73.0	72.4	71.7	71.1	70.6	70.0	69.4	68.8	68.3	67.7	67.2	66.7
B = 22	78.5	77.9	77.3	76.7	76.2	75.6	75.1	74.5	74.0	73.4	72.9	72.4	71.9	71.4	70.9	70.4	69.9	69.5	69.0	68.5
B = 24	78.6	78.1	77.6	77.1	76.6	76.1	75.7	75.2	74.7	74.3	73.8	73.4	73.0	72.5	72.1	71.7	71.3	70.8	70.4	70.0
B = 26	78.7	78.2	77.8	77.4	77.0	76.6	76.2	75.8	75.4	75.0	74.6	74.2	73.8	73.4	73.1	72.7	72.3	72.0	71.6	71.2
B = 28	78.7	78.4	78.0	77.6	77.3	76.9	76.5	76.2	75.9	75.5	75.2	74.8	74.5	74.2	73.8	73.5	73.2	72.9	72.5	72.2
B = 30	78.8	78.4	78.1	77.8	77.5	77.2	76.9	76.6	76.3	76.0	75.6	75.4	75.1	74.5	74.2	74.2	73.9	73.6	73.3	73.0
B = 32	78.8	78.5	78.2	78.0	77.7	77.4	77.1	76.9	76.6	76.3	76.1	75.8	75.5	75.3	75.0	74.7	74.5	74.2	74.0	73.7
B = 34	78.8	78.6	78.3	78.1	77.8	77.6	77.4	77.1	76.9	76.6	76.4	76.1	75.9	75.7	75.4	75.2	75.0	74.8	74.5	74.3
B = 36	78.9	78.6	78.4	78.2	78.0	77.8	77.5	77.3	77.1	76.9	76.7	76.5	76.2	76.0	75.8	75.6	75.4	75.4	75.0	74.8
B = 38	78.9	78.7	78.5	78.3	78.1	77.9	77.7	77.5	77.3	77.1	76.9	76.7	76.5	76.3	76.1	76.0	75.8	75.6	75.4	75.2
B = 40	78.9	78.7	78.5	78.4	78.2	78.0	77.8	77.6	77.5	77.3	77.1	76.9	76.8	76.6	76.4	76.3	76.1	75.9	75.7	75.6

Table 10. Propulsive efficiency $\eta_1 \times 10^2$ versus hydrodynamic resistance of submerged vehicle (Duct height $h = 4$ meters, duct width $w = 4$ meters, duct length $L = 10$ meters, hydrodynamic resistance $R = 2000\ V^2$ newtons. Velocity of submerged vehicle V in meters per second, magnetic induction B in tesla).

$V=$	2	4	6	8	10	12	14	16	18	20	22	24	26	28	30	32	34	36	38	40
$B=2$	31.8	19.6	14.1	11.1	9.1	7.7	6.7	5.9	5.3	4.8	4.4	4.0	3.7	3.5	3.3	3.1	2.9	2.7	2.6	2.5
$B=4$	59.7	46.2	37.7	31.8	27.5	24.2	21.7	19.6	17.9	16.4	15.2	14.1	13.2	12.4	11.7	11.1	10.5	10.0	9.5	9.1
$B=6$	71.3	61.7	54.4	48.6	44.0	40.1	36.9	34.2	31.8	29.7	27.9	26.3	24.9	23.6	22.5	21.4	20.5	19.6	18.8	18.0
$B=8$	76.5	69.9	64.4	59.7	55.6	52.1	49.0	46.2	43.7	41.5	39.5	37.7	36.0	34.5	33.1	31.8	30.6	29.5	28.5	27.5
$B=10$	79.2	74.5	70.4	66.7	63.4	60.4	57.7	55.2	52.9	50.8	48.8	47.0	45.4	43.8	42.3	41.0	39.7	38.5	37.4	36.3
$B=12$	80.7	77.3	74.2	71.3	68.6	66.2	63.9	61.7	59.7	57.8	56.1	54.4	52.8	51.4	50.0	48.6	47.4	46.2	45.1	44.0
$B=14$	81.6	79.1	76.6	74.4	72.2	70.2	68.3	66.4	64.7	63.1	61.5	60.1	58.6	57.3	56.0	54.8	53.6	52.5	51.4	50.4
$B=16$	82.3	80.3	78.3	76.5	74.7	73.1	71.5	69.9	68.5	67.1	65.7	64.4	63.2	62.0	60.8	59.7	59.6	57.6	56.5	55.6
$B=18$	82.7	81.1	79.5	78.0	76.6	75.2	73.8	72.5	71.3	70.1	68.9	67.8	66.7	65.6	64.4	63.6	62.6	61.7	60.8	59.9
$B=20$	83.0	81.7	80.4	79.2	78.0	76.8	75.6	74.5	73.5	72.4	71.4	70.4	69.5	68.5	67.6	66.7	65.9	65.0	64.2	63.4
$B=22$	83.3	82.2	81.1	80.0	79.0	78.0	77.0	76.1	75.2	74.2	73.4	72.5	71.7	70.8	70.0	69.2	68.5	67.7	67.0	66.3
$B=24$	83.4	82.5	81.6	80.7	79.8	79.0	78.1	77.3	76.5	75.7	74.9	74.2	73.4	72.7	72.0	71.3	70.6	69.9	69.3	68.6
$B=26$	83.6	82.8	82.0	81.2	80.5	79.7	79.0	78.3	77.6	76.9	76.2	75.5	74.9	74.2	73.6	73.0	72.4	71.8	71.2	70.6
$B=28$	83.7	83.0	82.3	81.6	81.0	80.3	79.7	79.1	78.4	77.8	77.2	76.6	76.1	75.5	74.9	74.4	73.8	73.3	72.7	72.2
$B=30$	83.8	83.2	82.6	82.0	81.4	80.8	80.3	79.7	79.2	78.6	78.1	77.6	77.0	76.5	76.0	75.5	75.0	74.5	74.1	73.6
$B=32$	83.9	83.3	82.8	82.3	81.8	81.3	80.7	80.3	79.8	79.3	78.8	78.3	77.9	77.4	76.9	76.5	76.0	75.6	75.2	74.7
$B=34$	83.9	83.4	83.0	82.5	82.1	81.6	81.1	80.7	80.3	79.8	79.4	79.0	78.6	78.1	77.7	77.3	76.9	76.5	76.1	75.7
$B=36$	84.0	83.5	83.1	82.7	82.3	81.9	81.5	81.1	80.7	80.3	79.9	79.5	79.1	78.8	78.4	78.0	77.7	77.3	76.9	76.6
$B=38$	84.0	83.6	83.3	82.9	82.5	82.1	81.8	81.4	81.1	80.7	80.4	80.0	79.7	79.3	79.0	78.6	78.3	78.0	77.6	77.3
$B=40$	84.1	83.7	83.4	83.0	82.7	82.4	82.0	81.7	81.4	81.0	80.7	80.4	80.1	79.8	79.5	79.2	78.9	78.6	78.3	78.0

Table 11. Propulsive efficiency $\eta_1 \times 10^2$ versus hydrodynamic resistance of submerged vehicle. (Duct height $h = 4$ meters, duct width $w = 4$ meters, duct length $L = 10$ meters, hydrodynamic resistance $R = 3000\ V^2$ newtons. Velocity of submerged vehicle V in meters per second, magnetic induction B in tesla).

$V=$	2	4	6	8	10	12	14	16	18	20	22	24	26	28	30	32	34	36	38	40
$B=2$	25.4	15.0	10.6	8.2	6.7	5.6	4.9	4.3	3.8	3.5	3.2	2.9	2.7	2.5	2.4	2.2	2.1	2.0	1.9	1.8
$B=4$	53.6	39.2	30.8	25.4	21.6	18.8	16.7	15.0	13.6	12.4	11.4	10.6	9.9	9.2	8.7	8.2	7.8	7.4	7.0	6.7
$B=6$	67.5	55.9	47.8	41.7	36.9	33.2	30.1	27.6	25.4	23.6	22.0	20.6	19.4	18.3	17.3	16.5	15.7	15.0	14.3	13.7
$B=8$	74.2	65.8	59.1	53.6	49.1	45.3	42.0	39.2	36.7	34.5	32.6	30.8	29.3	27.9	26.6	25.4	24.4	23.4	22.5	21.6
$B=10$	77.8	71.6	66.4	61.9	57.9	54.4	51.4	48.6	46.1	43.9	41.9	40.0	38.3	36.8	35.3	34.0	32.8	31.6	30.6	29.6
$B=12$	79.9	75.3	71.2	67.5	64.2	61.2	58.4	55.9	53.6	51.5	49.6	47.8	46.1	44.5	43.0	41.7	40.4	39.2	38.0	36.9
$B=14$	81.2	77.6	74.4	71.4	68.6	66.1	63.7	61.5	59.5	57.5	55.7	54.0	52.4	50.9	49.5	48.2	46.9	45.7	44.6	43.5
$B=16$	82.1	79.3	76.6	74.2	71.9	69.7	67.7	65.8	64.0	62.3	60.6	59.1	57.6	56.2	54.9	53.6	52.4	51.3	50.2	49.1
$B=18$	82.7	80.4	78.3	76.2	74.3	72.5	70.7	69.1	67.5	66.0	64.5	63.1	61.8	60.5	59.3	58.1	57.0	55.9	54.9	53.9
$B=20$	83.1	81.3	79.5	77.8	76.1	74.6	73.1	71.6	70.2	68.9	67.6	56.4	65.2	64.0	62.9	61.9	60.8	59.8	58.9	57.9
$B=22$	83.4	81.9	80.4	78.9	77.5	76.2	74.9	73.6	72.4	71.3	70.1	69.0	67.9	66.9	65.9	64.9	64.0	63.1	62.2	61.3
$B=24$	83.7	82.4	81.1	79.9	78.7	77.5	76.4	75.3	74.2	73.2	72.1	71.2	70.2	69.3	68.4	67.5	66.6	65.8	65.0	64.2
$B=26$	83.9	82.8	81.7	80.6	79.5	78.5	77.5	76.6	75.6	74.7	73.8	72.9	72.1	71.2	70.4	69.6	68.8	68.1	67.3	66.6
$B=28$	84.1	83.1	82.1	81.2	80.3	79.4	78.5	77.6	76.8	76.0	75.2	74.4	73.6	72.9	72.1	71.4	70.7	70.0	69.3	68.6
$B=30$	84.2	83.3	82.5	81.7	80.8	80.1	79.3	78.5	77.8	77.0	76.3	75.6	74.9	74.2	73.6	72.9	72.3	71.6	71.0	70.4
$B=32$	84.3	83.5	82.8	82.1	81.3	80.6	79.9	79.3	78.6	77.9	77.3	76.6	76.0	75.4	74.8	74.2	73.6	73.0	72.5	71.9
$B=34$	84.4	83.7	83.0	82.4	81.7	81.1	80.5	79.9	79.3	78.7	78.1	77.5	76.9	76.4	75.8	75.3	74.8	74.2	73.7	73.2
$B=36$	84.4	83.8	83.3	82.7	82.1	81.5	81.0	80.4	79.9	79.3	78.8	78.3	77.7	77.2	76.7	76.2	75.7	75.3	74.8	74.3
$B=38$	84.5	84.0	83.4	82.9	82.4	81.9	81.4	80.9	80.4	79.9	79.4	78.9	78.4	78.0	77.5	77.1	76.6	76.2	75.7	75.3
$B=40$	84.6	84.1	83.6	83.1	82.6	82.2	81.7	81.3	80.8	80.4	79.9	79.5	79.0	78.6	78.2	77.8	77.4	76.9	76.5	76.1

Table 12. Propulsive efficiency $\eta_1 \times 10^2$ versus hydrodynamic resistance of submerged vehicle. (Duct height $h = 4$ meters, duct width $w = 4$ meters, duct length $L = 10$ meters, hydrodynamic resistance $R = 4000\ V^2$ newtons. Velocity of submerged vehicle V in meters per second, magnetic induction B in tesla).

$V=$	2	4	6	8	10	12	14	16	18	20	22	24	26	28	30	32	34	36	38	40
$B=2$	21.1	12.1	8.4	6.5	5.3	4.4	3.8	3.4	3.0	2.7	2.5	2.3	2.1	2.0	1.8	1.7	1.6	1.5	1.5	1.4
$B=4$	48.3	33.8	26.0	21.1	17.8	15.4	13.5	12.1	10.9	9.9	9.1	8.4	7.9	7.3	6.9	6.5	6.1	5.8	5.5	5.3
$B=6$	63.4	50.7	42.2	36.2	31.7	28.2	25.3	23.0	21.1	19.5	18.1	16.9	15.8	14.9	14.1	13.3	12.7	12.1	11.5	11.0
$B=8$	71.2	61.5	54.1	48.3	43.6	39.8	36.5	33.8	31.4	29.4	27.6	26.0	24.6	23.3	22.2	21.1	20.2	19.3	18.5	17.8
$B=10$	75.5	68.1	62.1	57.1	52.8	49.1	45.9	43.1	40.6	38.4	36.4	34.6	33.0	31.5	30.2	28.9	27.8	26.7	25.8	24.8
$B=12$	78.0	72.4	67.6	63.4	59.6	56.3	53.4	50.7	48.3	46.1	44.1	42.2	40.5	39.0	37.5	36.2	35.0	33.8	32.7	31/7
$B=14$	79.6	75.3	71.4	67.9	64.7	61.8	59.1	56.7	54.5	52.4	50.5	48.7	47.0	45.5	44.0	42.7	41.4	40.2	39.1	38.0
$B=16$	80.7	77.3	74.1	71.2	68.5	65.9	63.6	61.5	59.4	57.5	55.7	54.1	52.5	51.0	49.6	48.3	47.0	45.8	44.7	43.6
$B=18$	81.5	78.7	76.1	73.6	71.3	69.1	67.1	65.2	63.4	61.7	60.0	58.5	57.0	55.6	54.3	53.1	51/8	50.7	49.6	48.5
$B=20$	82.0	79.7	77.5	75.5	73.5	71.6	69.8	68.1	66.5	65.0	63.5	62.1	60.8	59.5	58.3	57.1	56.0	54.9	53.8	52.8
$B=22$	82.5	80.5	78.7	76.9	75.2	73.6	72.0	70.5	69.1	67.7	66.4	65.1	63.9	62.7	61.6	60.5	59.4	58.4	57.4	56.5
$B=24$	82.8	81.1	79.5	78.0	76.5	75.1	73.7	72.4	71.2	69.9	68.7	67.6	66.5	65.4	64.4	63.4	62.4	61.5	60.5	59.6
$B=26$	83.0	81.6	80.2	78.9	77.6	76.4	75.2	74.0	72.9	71.8	70.7	69.7	68.7	67.7	66.7	65.8	64.9	64.0	63.2	62.4
$B=28$	83.2	82.0	80.8	79.6	78.5	77.4	76.3	75.3	74.3	73.3	72.3	71.4	70.5	69.6	68.7	67.9	67.1	66.2	65.5	64.7
$B=30$	83.4	82.3	81.3	80.2	79.2	78.2	77.3	76.4	75.5	74.6	73.7	72.8	72.0	71.2	70.4	69.6	68.9	68.1	67.4	66.7
$B=32$	83.5	82.6	81.6	80.7	79.8	79.0	78.1	77.3	76.4	75.6	74.9	74.1	73.3	72.6	71.9	71.2	70.5	69.8	69.1	68.5
$B=34$	83.6	82.8	82.0	81.1	80.3	79.6	78.8	78.0	77.3	76.6	75.8	75.1	74.5	73.8	73.1	72.5	71.8	71.2	70.6	70.0
$B=36$	83.7	83.0	82.2	81.5	80.8	80.1	79.4	78.7	78.0	77.3	76.7	76.1	75.4	74.8	74.2	73.6	73.0	72.4	71.9	71.3
$B=38$	83.8	83.1	82.5	81.8	81.1	80.5	79.9	79.2	78.6	78.0	77.4	76.8	76.3	75.7	75.1	74.6	74.0	73.5	73.0	72.5
$B=40$	83.9	83.3	82.7	82.0	81.5	80.9	80.3	79.7	79.2	78.6	78.1	77.5	77.0	76.5	76.0	75.5	74.9	74.5	74.0	73.5

Table 13. Propulsive efficiency $\eta_1 \times 10^2$ versus hydrodynamic resistance of submerged vehicle. (Duct height $h = 4$ meters, duct width $w = 4$ meters, duct length $L = 10$ meters, hydrodynamic resistance $R = 5000\ V^2$ newtons. Velocity of submerged vehicle V in meters per second, magnetic induction B in tesla).

V =	2	4	6	8	10	12	14	16	18	20	22	24	26	28	30	32	34	36	38	40
$B = 2$	18.0	10.1	7.0	5.4	4.4	3.7	3.2	2.8	2.5	2.2	2.0	1.9	1.7	1.6	1.5	1.4	1.3	1.3	1.2	1.1
$B = 4$	43.8	29.7	22.4	18.0	15.1	12.9	11.4	10.1	9.1	8.3	7.6	7.0	6.5	6.1	5.7	5.4	5.1	4.8	4.6	4.4
$B = 6$	59.5	46.2	37.8	31.9	27.7	24.4	21.8	19.7	18.0	16.6	15.4	14.3	13.4	12.6	11.8	11.2	10.6	10.1	9.6	9.2
$B = 8$	68.1	57.4	49.7	43.8	39.1	35.4	32.3	29.7	27.4	25.5	23.9	22.4	21.1	20.0	19.0	18.0	17.2	16.4	15.7	15.1
$B = 10$	72.9	64.7	58.2	52.8	48.4	44.6	41.4	38.6	36.2	34.0	32.1	30.4	28.9	27.5	26.3	25.1	24.1	23.1	22.2	21.4
$B = 12$	75.9	69.5	64.1	59.5	55.5	52.0	48.9	46.2	43.8	41.6	39.6	37.8	36.1	34.6	33.2	31.9	30.8	29.7	28.6	27.7
$B = 14$	77.8	72.7	68.3	64.4	60.9	57.8	55.0	52.4	50.1	48.0	46.0	44.2	42.5	41.0	39.5	38.2	36.9	35.8	34.7	33.6
$B = 16$	79.1	75.0	71.4	68.1	65.1	62.3	59.8	57.4	55.3	53.3	51.4	49.7	48.1	46.5	45.1	43.8	42.5	41.3	40.2	39.1
$B = 18$	80.0	76.7	73.6	70.8	68.2	65.8	63.6	61.5	59.5	57.7	55.9	54.3	52.8	51.3	49.9	48.6	47.4	46.2	45.1	44.0
$B = 20$	80.6	77.9	75.3	72.9	70.7	68.6	66.6	64.7	62.9	61.3	59.7	58.2	56.7	55.4	54.1	52.8	51.6	50.5	49.4	48.4
$B = 22$	81.1	78.8	76.6	74.6	72.6	70.8	69.0	67.4	65.8	64.2	62.8	61.4	60.1	58.8	57.6	56.4	55.3	54.2	53.2	52.2
$B = 24$	81.5	79.5	77.7	75.9	74.2	72.6	71.0	69.5	68.1	66.7	65.4	64.1	62.9	61.7	60.6	59.5	58.5	57.4	56.5	55.5
$B = 26$	81.8	80.1	78.5	76.9	75.4	74.0	72.6	71.3	70.0	68.8	67.6	66.4	65.3	64.2	63.2	62.2	61.2	60.2	59.3	58.4
$B = 28$	82.0	80.6	79.1	77.8	76.5	75.2	73.9	72.7	71.6	70.5	69.4	68.3	67.3	66.3	65.4	64.4	63.5	62.6	61.8	60.9
$B = 30$	82.2	80.9	79.7	78.5	77.3	76.2	75.1	74.0	72.9	71.9	70.9	70.0	69.0	68.1	67.2	66.4	65.5	64.7	63.9	63.1
$B = 32$	82.4	81.2	80.1	79.1	78.0	77.0	76.0	75.0	74.1	73.2	72.3	71.4	70.5	69.7	68.9	68.1	67.3	66.5	65.8	65.1
$B = 34$	82.5	81.5	80.5	79.5	78.6	77.7	76.8	75.9	75.0	74.2	73.4	72.6	71.8	71.0	70.3	69.5	68.8	68.1	67.4	66.8
$B = 36$	82.6	81.7	80.8	80.0	79.1	78.3	77.5	76.7	75.9	75.1	74.4	73.6	72.9	72.2	71.5	70.8	70.2	69.5	68.9	68.2
$B = 38$	82.7	91.9	81.1	80.3	79.5	78.8	78.0	77.3	76.6	75.9	75.2	74.5	73.9	73.2	72.6	72.0	71.3	70.7	70.1	69.5
$B = 40$	82.8	82.0	81.3	80.6	79.9	79.2	77.2	76.6	75.9	75.3	74.7	74.1	73.5	72.9	72.4	71.8	72.4	71.8	71.2	70.7

DISCUSSION AND CONCLUSIONS

A simple magnetohydrodynamic (MHD) propulsive configuration can be a straight rectangular duct employed to produce the thrust for a submerged vehicle. The MHD propulsive duct can be within the hull of the submerged vehicle, in the configuration of a "pod" attached by struts to the main vehicle, or in an array around the outside surface of the vehicle. In the mathematical model discussed herein, the friction on the duct walls due to fluid flow was approximately represented by the ordinary smooth pipe flow frictional formulation. The vertical duct walls contained electrodes, the horizontal walls contained superconducting magnets, and the duct wall thickness was assumed to be zero. Neither the power supplied to the duct's superconducting magnet configuration nor the magnet masses were considered in the mathematical model. End effects, which degrade propulsive efficiency, and bubble generation, were also omitted.

The fundamental rectangular duct MHD propulsion system was mathematically modelled to compute the propulsive efficiencies of the system. The propulsive efficiency of the duct within the hull of the vehicle was designated as η_1; the propulsive efficiency of the duct as an external pod was designated as η_2. The propulsive efficiency $\eta_2 < \eta_1$ because of the increased skin friction of the system due to the external skin friction of the pod. Numerical solutions were presented for the propulsive efficiencies η_1 and η_2 of the MHD propulsion duct in regard to such variables as duct geometry, duct magnetic induction, electrical conductivity of fluid, submerged vehicle speed, submerged vehicle hydrodynamic drag, and skin friction fluid drag inside the duct.

The propulsive efficiencies calculated from the model in general overestimate the efficiencies of the corresponding real MHD propulsion system. The numerical propulsion efficiency curves in this report can be used for engineering estimates of the propulsive efficiencies of real MHD propulsion systems.

In this work, a base MHD duct was chosen with width 4 meters, height 4 meters, length 10 meters, and magnetic induction of .6 tesla across the duct propelling a submerged vehicle of 3,000 V^2 newtons at a vehicle speed of 10 meters per second. The propulsive efficiencies η_1 and η_2 related to the base MHD propulsive duct propelling the submerged vehicle have the following properties:

- In a 6 tesla field η_1 and η_2 decrease from 0.67 and 0.61 at 2.0 meters per second to 0.24 and 0.22 at 20.0 meters per second, respectively, a significant decrease in efficiency with increasing vehicle speed.
- At a constant vehicle speed of 10 meters per second η_1 and η_2 increase from 0.07 and 0.06 at 2 tesla to 0.67 and 0.63 at 14 tesla , respectively, a significant increase in efficiency with magnetic induction.
- η_1 and η_2 increase from 0.07 and 0.06 at an electrical conductivity of seawater of 0.4 siemens per meter to 0.67 and 0.62 at conductivity of 20.0 siemens per meter, respectively, a significant increase in efficiency with seawater electrical conductivity. If possible at all, the conductivity of the seawater in the duct could be increased in practice only by "seeding." (The

electrical conductivity of seawater is on the average approximately 4 siemens per meter.)

- At a constant vehicle speed of 10 meters per second and a magnetic induction of 6 tesla, η_1 and η_2 increase from 0.14 and 0.13 at a duct cross section of 4 meters^2 to 0.62 and 0.53 at a cross section of 64 meters^2
- At 6 tesla η_1 and η_2 increase from 0.13 and 0.12 at a duct length of 2.0 meters to 0.46 and 0.39 at duct length of 20.0 meters, respectively, a significant increase in efficiency with moderate duct length at 6 tesla. Increasing the duct length to 200 meters deceases η_1 to 0.30, as would be expected because of the increased skin friction inside an extremely long duct.
- At vehicle speed of 10 meters per second, magnetic induction of 6 tesla, and duct length 10 meters, η_1 increases from 0.24 to 0.43 with an increase in the electrode height (i.e., duct height) from 4 meters to 32 meters, a significant increase in efficiency with electrode height.
- At vehicle speed of 10 meters per second, magnetic induction of 6 tesla, duct height of 4 meters, and duct length of 10 meters, η_1 increases from 0.14 at a duct width of 1 meter (i.e., distance between electrodes) to 0.60 at a width of 16 meters, a significant increase in efficiency.
- At a vehicle speed of 10 meters per second, η_1 generally decreases with increases in the hydrodynamic resistance of the submerged vehicle from 1000 V^2 newtons to 5000 V^2 newtons.

Thus, in summary, according to the mathematical model presented here and the range of parameters studied, the ideal MHD propulsive duct efficiencies increase in magnitude with increase in the following factors: channel magnetic induction, square duct cross sectional area at moderate duct lengths, fluid electrical conductivity, duct length, distance between electrodes, and electrode height.

The ideal MHD propulsive efficiencies decrease with vehicle speed, and generally decrease with increasing vehicle hydrodynamic drag. Extremely long ducts significantly decrease propulsive efficiencies because of the increase in internal duct friction.

A comparison of the ideal MHD propulsive efficiencies η_1 and η_2 for a submerged vehicle with the corresponding efficiencies of a conventional propeller* (i.e., 0.85), generally shows the MHD efficiencies to be less under most conditions. The MHD efficiencies η_1 and η_2 which approach that of a propeller correspond to ducts of very large volumes (order of magnitude of 300 meters^3 with small surface to volume ratios), or require very high duct field values (20 or 25 tesla). In large volumes of space such as MHD ducts, magnetic inductions of about 6 to 10 tesla are about the highest field strengths possible with the use of present day superconducting magnet construction tech-

* McCarthy, J.N., Head, Naval Hydromechanics Division at DTRC (Code 154), Private communication (Oct 1989).

nology,** and producing these fields would require a significant engineering effort in magnet construction.

MHD propulsive ducts have no mechanical moving parts and consequently may produce less acoustic noise than propellers under the same propulsion conditions. Also, not having a propeller removes the problem of propeller hull shaft seals. *Using MHD propulsion on a submerged vehicle to reduce the acoustic signature as compared with a conventional propeller-driven vehicle is possibly a very promising feature, and it should be investigated, even though the MHD system generally has a lower propulsive efficiency. Therefore, it should be determined if the MHD propulsion technology is available or can be developed in the future to build a submerged vehicle that produces less acoustic noise then conventional submerged vehicles.*

ACKNOWLEDGMENTS

The authors would like to thank L.J. Argiro, H.O. Stevens, M.J. Superczynski, R.C. Smith, and D. B. Larrabee, all of DTRC, for many helpful technical discussions and much encouragement while this work was in progress. Also, we would like to express our appreciation to Dr. W. J. Levedahl, of DTRC, for many helpful discussions involving the mathematical modelling. The work was also supported by many technical discussions with Dr. Kenneth Tempelmeyer, Secretary of the Navy Fellow at the U.S. Naval Academy during 1989 and Professor at the College of Engineering at Southern Illinois University.

** Superczynski, M.J., Superconductive Project Coordinator at DTRC, Private Communication (Apr 1989).

APPENDIX A
THREE-DIMENSIONAL EFFECTS

This report presents a one-dimensional control-volume model for an MHD duct which is moving through an unbounded fluid and which is accelerating part of that fluid so as to develop forward thrust. In this model, the velocity has only an axial component, while the velocity and pressure are uniform across each cross section of the flow. Clearly, the flow upstream and downstream of the duct must actually have three nonzero velocity components, not one; neither are the pressure and velocity uniform across each cross section. The present model is an approximate extension of the one-dimensional model for a propellor in an open sea. The key difference between the two applications is that the open-sea propellor provides a pressure rise across a disk of essentially zero thickness with no other solid surfaces, while the MHD duct provides a pressure rise over the axial length L of the duct. The effect of the finite-length duct walls is very similar to the effect of a cylinder or shroud placed around a propellor. This effect is treated in detail by Kuchemann and Weber.[25] Here we only summarize the key features and their implications for the MHD propulsion duct.

The propellor alone in an open sea creates a certain two-dimensional, axisymmetric flow with a radially inward flow associated with the axial acceleration. If a cylinder of finite length is placed around the propellor, it locally blocks the radial velocity component. In essence, each section of the cylinder acts as an airfoil in the radially converging flow created by the propellor alone. To be an effective airfoil, the flow must not separate at the leading edge of the cylinder and this dictates a minimum radius of curvature of the wall here. In other words, the wall of the cylinder cannot be too thin at the front.

The effects of the cylinder as an airfoil can be stated in several equivalent ways. First, we can say that the circulation associated with the airfoil section increases the flow through the propellor. For a given thrust, the increase in velocity is smaller with more flow, so that there is less kinetic energy lost in the jet aft of the propellor. An ideal shroud always increases the efficiency, but an actual shroud adds skin-friction drag, which to some degree offsets the gain, depending on the particular case. A second way to describe the effect of the cylinder is to say that the airfoil produces a pressure on the forward, inside surface of the cylinder which is further below the ambient pressure than the local pressure would be without the cylinder. This lower pressure has two effects. First, it draws more fluid into the cylinder, resulting in more flow through the propellor. Second, the propellor still provides an increase in pressure, but now the upstream pressure is further below ambient pressure, so that the exit pressure is not as far above ambient pressure. As a result, the jet aft of the propellor does not accelerate and contract as much, so again there is less kinetic energy lost.

The cylinder cannot be treated as an airfoil in the open-sea propellor flow. The presence of the cylinder changes the flow created by the propellor, so that the airfoil-cylinder and the pressure-jump propellor disk must be treated together. For axisymmetric shrouded propellors, Kuchemann and Weber[25] present solutions involving axisymmetric vortex sheets which produce flows satisfying the boundary conditions at the shroud walls and at the propellor disk. The thrust is now divided between the propellor and shroud or cylinder. The propellor thrust is still equal to the pressure increase times the disk area. The pressures which are below the ambient pressure near the leading edge of the cylinder or shroud produce an additional forward thrust on the cylinder. An airfoil alone would

have no net axial force. However, the propellor produces an abrupt pressure jump on the inside surface of the airfoil-cylinder. Thus the pressures on the forward and aftward parts of the airfoil are lower and higher, respectively, than they would be without the propellor, and there is a net force on the cylinder or shroud. If the cylinder wall has zero thickness and if the leading edge separation is erroneously ignored, then the pressure at the leading edge is minus infinity. This infinite negative pressure acting over the zero area of the leading edge gives the finite forward thrust on the cylinder.

The MHD equivalent of an open-sea propellor would be a uniform axial body force, JB, acting over the rectangular volume of length L, but with no duct walls. The streamlines which would result from such an open-sea body force distribution are sketched in Fig. 19 The forward thrust on the ship associated with this acceleration would be applied to the magnet coils producing the magnetic field. When we add the actual duct walls, they locally block the transverse velocity components and therefore act as airfoils with inward lift forces. There is now an additional forward thrust on the duct walls, associated primarily with the much lower pressures near the entrance associated with the circulation produced by the airfoil-duct walls. Again the duct walls would require a finite thickness and minimum radius of curvature to prevent separation at the entrance. Indeed, there would certainly be fairings fore and aft of the straight duct walls since straight walls alone would not represent the optimal airfoil cross sections.

The two-dimensional, axisymmetric analysis of Kuchemann and Weber[25] for a shrouded propellor cannot be extended to the MHD duct in a straightforward fashion. First, the pressure jump across the zero-thickness propellor is replaced by a distributed body force. Second, the flow is in general three-dimensional, although some designs for

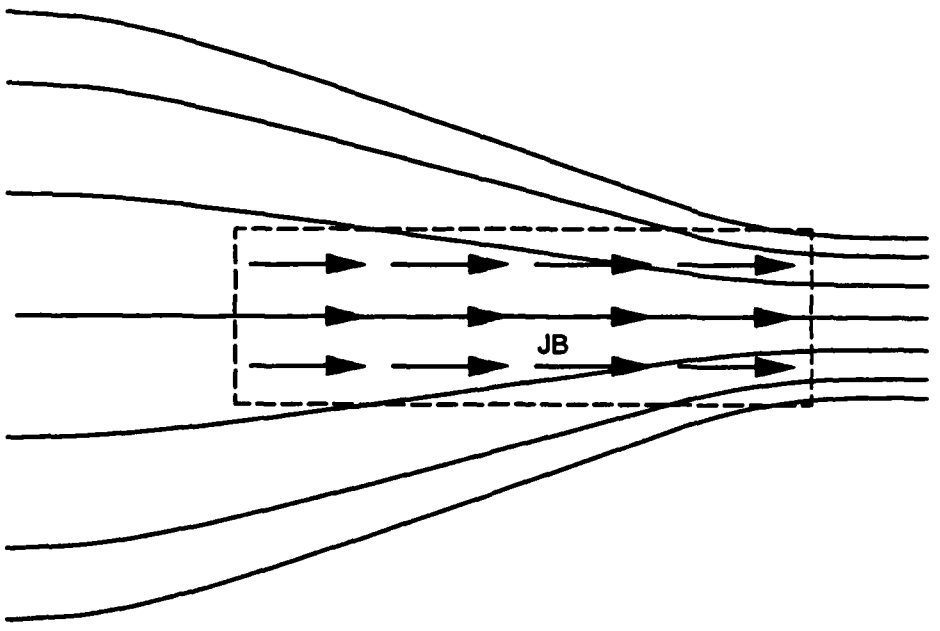

Fig. 19. Streamlines due to uniform body force *JB* distributed over rectangular volume with no duct walls.

the MHD propulsion of submerged vehicles might involve axisymmetric flows. Since a new two- or three-dimensional analysis would by needed to treat the effect of the duct walls, it would be inappropriate to keep a one-dimensional model of the MHD body force. One would want to include the effects of the spatially decaying, fringing magnetic fields and electric currents near the entrance and exit. We have not presented such a two- or three-dimensional model here. Our present purpose was to provide the best predictions possible with a one-dimensional model.

While we have not determined the increase in the flow through the duct due to the airfoil effect of the duct walls, we can make a few qualitative statements based on the results of Kuchmenn and Weber. They treated a propellor at the middle of a long cylinder and found that the cylinder increases the velocity at the propellor. The effect on the energy balance for a fixed ship velocity and total thrust is to decrease the kinetic energy lost aft of the propellor. For most of the cases considered here, the lost kinetic energy was relatively small compared to other losses, particularly Joulean heating. Therefore, even a relatively large reduction on the lost kinetic energy may not significantly improve the overall efficiency of the propulsion unit. In addition, an increase in the velocity inside the duct increases the frictional losses, which vary as the square of the duct velocity, so that any gains are offset to a degree which depends on the particular case.

REFERENCES

1. Blake, L.R., "Conduction and Induction Pumps for Liquid Metals," *The Proceedings of the Institution of Electrical Engineers*, Part A, pp. 49–63; discussion pp. 63–67 (February 1957).

2. Cage, J.F. Jr., "Electromagnetic Pumps for High–Temperature Liquid Metal," *Mechanical Engineering*, pp. 467–471 (June 1953).

3. Barnes, A.H. and J.F. Cage, Jr., "Pumps–Electromagnetic, " *Liquid Metals Handbook, Sodium-NaK Supplement*, pp. 288–305 (1 July 1955).

4. Way, S., "Propulsion of Submarines by Lorentz Forces in the Surrounding Sea," American Society of Mechanical Engineers, ASME Paper 64 WA/ENER7 (Nov 1964).

5. Way, S. and C. Devlin, "Prospects for the Electromagnetic Submarine, "AIAA 3rd Propulsion Joint Specialist Conference, AIAA Paper 67–432 (July 17–21, 1967).

6. Way, S. and C. Devlin, "Construction and Testing of a Model Electromagnetically Propelled Submarine," *Proceedings*, Eighth Symposium on the Engineering Aspects of Magnetohydrodynamics, Stanford University, California, pp. 153–154 (March 28–30, 1967).

7. Way, S., "Electromagnetic Propulsion for Cargo Submarine," *Journal of Hydronautics*, Vol . 2, No. 2, pp. 49–57 (April 1968).

8. Doragh, R.A., "Magnetohydrodynamic Ship Propulsion Using Superconducting Magnets," Society of Naval Architects and Marine Engineers, *SNAME Transactions*, Vol. 71, pp. 370–386 (1963).

9. Friauf, James B., "Electromagnetic Ship Propulsion," American Society of Naval Engineers, *ASNE Journal*, pp. 139–142 (February 1961).

10. Phillips, O.M., "The Prospects for Magneto-Hydrodynamic Ship Propulsion," *Journal of Ship Research*, Vol. 5, No. 4, pp. 43–51 (March 1962).

11. Resler, E.L. Jr., "Magnetohydrodynamic Propulsion for Sea Vehicles," Seventh Symposium on Naval Hydrodynamics, Rome, Italy, pp. 1437–1445 (1968)

12. Vasil'ev A.P. and I.M. Kirko, "Optimization of a Marine MHD Propeller," Translated from *Zhurnal Prikladnoi Mekhanikii Tekhnicheskoi Fiziki*, No. 3, pp. 86–94 (May–June 1981).

13. Yakovlev, V.I., "Theory of an Induction MHD Propeller With a Free Field," Translated from *Zhurnal Prikladnoi Mekhanikii Tekhnickeskoi Fiziki*, No. 3, pp. 105–116 (May–June 1980).

14. Mitchell, D.L. and D.U. Gubser, *Journal of Superconductivity*, Vol. 1 (1988).

15. Saji, Y., M. Kitano, and A. Iwata, *Advanced Cryogenic Engineering*, Vol. 23 (1978).

16. Iwata, A., E. Tada, and Y. Saji, "Experimental and Theoretical Study of Superconducting Electromagnetic Ship Propulsion," 5th LIPS Propeller Symposium, No. 2 (1983).

17. Iwata, A., Y. Takeda, and Y. Saji, *Journal of Marine Engineering of Japan*, Vol. 16 (1982).

18. Walker, J.S., S.H. Brown, and N.A Sondergaard, *Journal of Applied Physics*, Vol. 64 No. 1 (July 1988).

19. Walker, J.S., S.H. Brown, and N.A. Sondergaard, *Journal of Applied Physics*, Vol. 64 No. 4 (15 August 1988).

20. Hughes, W.F. and I.R. McNab, "A Quasi-One-Dimensional Analysis of an Electromagnetic Pump Including End Effects," *Liquid-Metal Flows and Magnetohydrodynamics*, H. Branover, A. Yakot, and P.S. Lykoudis, eds., Vol. 84 of *Progress in Astronautics and Aeronautics* (1983).

21. Attwood, E.L. and H.S. Pengelly, *Theoretical Naval Architecture*, Longmans, Green and Co. Ltd., London, England (1953).

22. Hughes, W.F. and F.J. Young, *The Electromagnetodynamics of Fluids*, John Wiley and Sons, Inc., New York (1966).

23. Landau, L.D. and E.M. Liftshitz, *Fluid Mechanics*, Pergamon Press, Addison–Wesley Publishing Co., Inc., Reading Massachusetts (1959).

24. Shercliff, J.A., *A Textbook of Magnetohydrodynamics*, Pergamon Press, New York (1965).

25. Kuchemann, Dietrich and Johanna Weber, *Aerodynamics of Propulsion*, McGraw Hill, New York (1953).

INITIAL DISTRIBUTION

Copies

3 DARPA/STP
LCDR Richard Martin
Advanced Technology
1515 Wilson Blvd., Suite 705
Arlington, VA 22209

2 Gene Remmers
Office of Chief of Naval Research
Office of Naval Technology
800 N. Quincy St.
Arlington, VA 22217–5000

12 DTIC

20 Dr. John S. Walker
University of Illinois at
Urbana-Champaign
Dept. Mech. & Ind. Engineering
144 Mechanical Engineering Bldg
1206 West Green St.
Urbana, IL 61801

3 Dr. Daniel W. Swallom
Avco Research Lboratory
2385 Revere Beach Parkway
Everett, MA 02149

3 Dr. Michael Petrick
Argonne National Laboratory
9700 South Cass Ave.
Argonne, IL 60439

3 Dr. Kenneth E. Tempelmeyer
c/o Office of the Dean
College of Engineering and
Technology
Southern Illinois University
Carbondale, IL 62901

3 Dr. Basil Picologlou
Engineering Physics Division
Argonne National Laboratory
9700 South Cass Ave.
Argonne, Illinois 60439

CENTER DISTRIBUTION

Copies	Code	Name
3	01	Richard E. Metry
3	0113	Dr. Bruce E. Douglas
3	154	Justin H. McCarthy
3	1544	Dr. Frank B. Peterson
2	1561	Geoffrey Cox
2	1942	Dr. Theodore M. Farabee
2	27	Larry J. Argiro
2	2752	Robert J. Chomo
2	2701	James L. Corder
5	2702	Dr. William Levedahl
2	2704	Dr. Earl Quandt, Jr.
2	271	Howard O. Stevens, Jr.
10	2711	David E. Bagley
2	2711	Robert C. Smith
10	2712	Dr. Samuel H. Brown
10	2712	Patrick J. Reilly
10	2712	Dr. Neal A. Sondergaard
2	2712	Michael J. Supercznyski, Jr.
2	272	Timothy J. Doyle
2	2720	Dr. Herman Urbach
2	2743	David B. Larrabee
2	275	Dr. Cyril Krolick
3	2772	John G. Stricker
2	2812	Louis F. Aprigliano
1	3411	Margaret L. Knox
1	3421	TIC Carderock
2	3422	TIC Annapolis